

TOWARDS A STATIONARY MONGE-KANTOROVICH DYNAMICS: THE PHYSARUM POLYCEPHALUM EXPERIENCE

ENRICO FACCA, FRANCO CARDIN AND MARIO PUTTI

ABSTRACT. In this work we study and expand a model describing the dynamics of a unicellular slime mold, *Physarum Polycephalum* (PP), which was proposed to simulate the ability of PP to find the shortest path connecting two food sources in a maze. The original model describes the dynamics of the slime mold on a finite dimensional planar graph using a pipe-flow analogy whereby mass transfer occurs because of pressure differences with a conductivity coefficient that varies with the flow intensity. We propose an extension of this model that abandons the graph structure and moves to a continuous domain. The new model, that couples an elliptic equation enforcing PP density balance with an ODE governing the dynamics of the flow of information along the PP body, is analyzed by recasting it into an infinite-dimensional dynamical system. We are able to show well-posedness of the proposed model for sufficiently small times under the hypothesis of Hölder continuous diffusion coefficients and essentially bounded forcing functions, which play the role of food sources. Numerical evidence, shows that the model is capable of describing the slime mold dynamics also for large times, accurately reproducing the PP behavior.

A notable result related to the original model is that it is equivalent to an optimal transportation problem over the graph as time tends to infinity. In our case, we can only conjecture that our extension presents a time-asymptotic equilibrium. This equilibrium point is precisely the solution of the Monge-Kantorovich (MK) equations at the basis of the PDE formulation of optimal transportation problems. Numerical results obtained with our approach, which combines \mathcal{P}_1 Finite Elements with forward Euler time stepping, show that the approximate solution converges at large times to an equilibrium configuration that well compares with the numerical solution of the MK-equations.

Slime-mold dynamics; MongeKantorovich transport problem; Dynamic formulation; Numerical solution.

[2000] 49K20,49M25,35J70,65N30

1. INTRODUCTION

In a recent paper, Tero et al. [18] proposed a mathematical model governing the dynamics of a unicellular slime mold named *Physarum Polycephalum* (PP) that, on the basis of experimental evidence [17], grows following the most efficient network path between food sources. This evidence is exemplified in the picture shown in Fig. 1 that portrays the experimental setup developed by Nakagaki et al. [17] suggesting that *Physarum* slime, after colonization of the entire maze paths, evolves along the shortest path connecting the two food sources. *P. Polycephalum* abilities have been used for the experimental analysis of transportation networks, with many researchers suggesting that this slime mold is capable of identifying the optimal many-site connecting transportation network, with applications to such systems as the railroads of Tokyo and Spain [1, 19]. Many further surprising properties of PP have been experimentally identified, but in this work we are interested in studying and extending the mathematical model proposed by Tero et al. [18] that governs the slime mold dynamics.

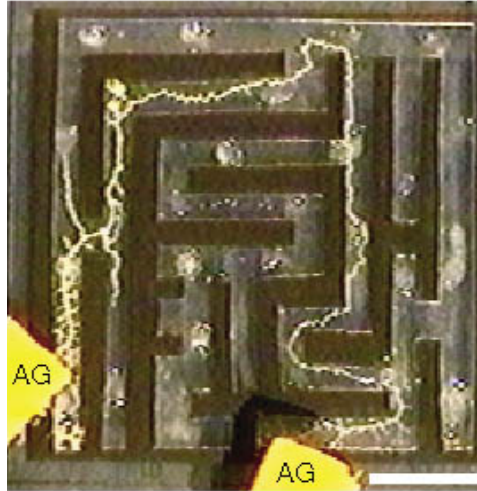


FIGURE 1. *Physarum Polycephalum* experimental maze solving (from Nakagaki et al. [17])

The original model of Tero et al. [18] reads as follows. Given a undirected planar graph $G = (E, V)$, with positive edge length $\{L_e\}_{e \in E}$ find the edge function D_e and the vertex function p_v that satisfy:

$$\begin{aligned}
 (1a) \quad & \sum_{e \in \sigma(v)} Q_e(t) = f_v \quad (\text{“Balance law-Kirchhoff”}) & \forall v \in V, \\
 (1b) \quad & Q_e(t) = D_e(t) \frac{(p_u(t) - p_v(t))}{L_e} \quad (\text{“Fick-Poiseuille”}) & \forall e = (u, v) \in E, \\
 (1c) \quad & D'_e(t) = g(|Q_e(t)|) - D_e(t) \quad (D_e \text{ dynamics}) & \forall e = (u, v) \in E, \\
 (1d) \quad & D_e(0) = \hat{D}_e(0) > 0 \quad (\text{initial data}) & \forall e = (u, v) \in E,
 \end{aligned}$$

where $e = (u, v)$ denotes the edge of G connecting vertices u and v , the vertex source function f_v satisfies the compatibility condition of an isolated system $\sum_{v \in V} f_v = 0$ [6], where $\sigma(v)$ is the “star” of v , i.e., the set of edges having vertex v in common and $g : \mathbb{R}^+ \mapsto \mathbb{R}^+$ is a non-decreasing function with $g(0) = 0$. This model can be explained heuristically using a classical hydraulic analogy, eventually motivating the above introduced terms “balance law-Kirchhoff” and “Fick-Poiseuille”. We think of the graph G as representing the set of pipes where the flow of a fluid driven by the vertex source function f_v occurs. Then, the first equation (1a) can be identified as the enforcement of the fluid mass balance, while equation (1b) is the momentum balance stating that the flux in each graph edge is proportional to the discrete gradient of the vertex potential function p_v (1b) via a conductance coefficient D_e (inverse of a resistance). Hydraulic resistance to flow is known to be proportional to the pipe perimeter, and hence to its diameter. Thus, the evolutive equation (1c), which forms the core of the model, asserts the intuitive behavior that to optimally (with minimal energy loss) accommodate larger fluxes, the pipe diameter must increase, although it needs to remain bounded. From this observation it can be concluded that the function $g(x)$ must be nondecreasing. Moreover, to avoid unboundedness, the growth of the hydraulic conductivity needs to be compensated by introducing the balancing decay term $-D_e(t)$. In Tero et al. [18] several numerical results using this model were presented. The most relevant to our study are those where the vertex source function was concentrated in the first (1) and last (n) vertex of the graph (the entrance and exit of the fluid in the

hydraulic analogy), i.e.:

$$f_v = \begin{cases} +1 & v = 1 \\ -1 & v = n \\ 0 & \text{otherwise} \end{cases}$$

Using this setting, the numerical evidence shows that when $g(x) = x$ the conductivity D_e at large times tends to localize (have a nonzero support) on the edges of the shortest path between the two external sources. This has been confirmed more recently by Bonifaci et al. [6], who show that, for $t \rightarrow \infty$, indeed the distribution of D_e converges to the shortest path. Moreover, the same authors prove that the above model is equivalent to an optimal transport problem on the graph G and can be recasted as the problem of finding $Q = \{Q_e\}_{e \in E}$ such that:

$$\begin{aligned} \min_{Q \in \{Q_e\}_{e \in E}} J(Q), \quad J(Q) &:= \sum_{e \in E} Q_e L_e \\ \text{s.t.:} \\ \sum_{e \in \sigma(v)} Q_e &= f_v \quad \text{for all } v \in V. \end{aligned}$$

In fact, under some general assumptions on the graph structure, the solution of system (1) converges to a stationary solution Q that is also solution of the above optimal transport problem in G .

In this work we generalize the model given in (1) by removing the graph structure and defining the problem on an open bounded domain $\Omega \subset \mathbb{R}^n$. We restrict this study to the case of $g(x) = x$. Then, given a source function $f : \Omega \rightarrow \mathbb{R}$, a continuous analogue of (1) tries to find the pair of functions $(\mu, u) : [0, +\infty[\times \Omega \mapsto \mathbb{R}^+ \times \mathbb{R}^n$ that satisfies:

$$(2a) \quad -\nabla \cdot (\mu(t, x) \nabla u(t, x)) = f(x) \quad \left(\int_{\Omega} f \, dx = 0 \right)$$

$$(2b) \quad \mu'(t, x) = \mu(t, x) (|\nabla u(t, x)| - 1)$$

$$(2c) \quad \mu(0, x) = \mu_0(x) > 0$$

complemented by zero Neumann boundary conditions. Here, μ' indicates partial differentiation with respect to time, and $\nabla = \nabla_x$. This generalization is intuitively justified by comparing the different components of models (1) and (2). In fact, (2a) states the spatial balance of a (continuum) Fick-Poiseuille flux $q = -\mu \nabla u$ with potential function u , while (2b) introduces the dynamics introduced in the original discrete model. To address the dynamics of PP in the maze, we need to reconcile the model with the fact that some portions of the domain (the maze barriers in this case) may hinder through-flow. This can be obtained by imposing the gradient to be large where the flux must be small, thus forcing the conductivity μ to become small. Thus, equation (2b) is replaced by:

$$(3) \quad \mu'(t, x) = \mu(t, x) (|\nabla u(t, x)| - k(x))$$

where $k(x)$ is a positive function describing the spatial pattern of the resistance to flow, whereby large values of k imply large energy losses and hence large gradients of the potential u . Note that, intuitively, since the flux q must remain bounded, larger gradients induce smaller conductivities and hence smaller fluxes.

In the present paper, we analyze from an analytical and numerical point of view the continuous model of slime-mold dynamics described above, and we conjecture that, like its discrete counterpart, its solution tends to an equilibrium point as time goes to infinity and that this equilibrium point is the solution of the Monge-Kantorovich optimal mass transport problem [13]. We first study existence

and uniqueness of the solution of (2) for the case $k \equiv 1$, as the more general case with heterogeneous $k(x)$ is a straight forward adaptation, at least for smooth enough k . For $k \equiv 1$, if an equilibrium point exists for $t \rightarrow +\infty$, then $\mu' \rightarrow 0$. Hence, (2b) becomes a constraint imposing that for, μ strictly greater than or equal to zero, the norm of the gradient of u must be unitary. This observation is crucial to the development of our conjecture, which reads as:

Conjecture 1. *The solution of (2) tends as $t \rightarrow \infty$ to the solution of the following problem: find $(\mu^*, u^*) \in (L^\infty(\Omega), Lip_1(\Omega))$, with $Lip_1(\Omega)$ the space of Lipschitz continuous functions with unit constant, such that:*

$$(4) \quad \begin{aligned} -\nabla \cdot (\mu^*(x) \nabla u^*(x)) &= f^+(x) - f^-(x) = f(x) && \text{in } \Omega \\ |\nabla u^*(x)| &\leq 1 && \text{in } \Omega \\ |\nabla u^*(x)| &= 1 && \text{where } \mu^*(x) > 0 \end{aligned}$$

These equations constitute the PDE-based formulation of the classical optimal transport problem and are named the *Monge-Kantorovich* (MK) equations [2, 7, 13]. In the past few years they have been the subject of a number of studies that have shed light into regularity and integrability properties of the *optimal transport density* μ^* in relation to the regularity and integrability of the forcing function f [12], and its uniqueness [14].

In this work we show the applicability of the proposed model to the simulation of the dynamics of *Physarum Polycephalum*, but, most notably, we try to point out to some theoretical and numerical evidence in support of veridicity of the above conjecture. From a theoretical point of view, we first prove the local-in-time existence and uniqueness of the solution pair (μ, u) in Hölder spaces. To this aim, we recast the problem in operatorial form and look for the functions $u(t)$ and $\mu(t)$ such that:

$$(5a) \quad \int_{\Omega} \mu(t) \nabla u(t) \nabla \varphi(x) dx = \int_{\Omega} f \varphi(x) dx \quad \forall \varphi \in H^1(\Omega)$$

$$(5b) \quad \mu'(t) = \mathcal{Q}(\mu(t)) - \mu(t); \quad \mu(0) = \mu_0$$

where $\mathcal{Q}(\mu)$ is the operator, associated with the weak form (5a) of the elliptic PDE (2a), that maps μ into $\mu|\nabla u|$. To simplify notation, we consider the dependence on $x \in \Omega$ implicit in all the relevant functions. For a given $\mu > 0$, we denote by $\mathcal{U}(\mu)$ the unique weak solution of the elliptic PDE associated with μ . Clearly, the solution $\mu(t)$ remains bounded as long as the left-hand-side remains negative, i.e., $|\nabla \mathcal{U}(\mu(t))| \leq 1$. Standard regularity theory of elliptic PDEs ensures that, for any source function $f \in L^\infty(\Omega)$ the operator $\mathcal{Q}(\mu)$ is well-defined (meaning problem (2a) is well-posed, i.e., the associated bilinear form is coercive and continuous) for $\mu(t, x)$ Hölder continuous and strictly greater than zero. We are then able to show that the operator $\mathcal{Q}(\mu)$ is locally Lipschitz continuous, and we can then invoke Banach-Caccioppoli fixed-point theorems to show local existence and uniqueness of the solution pair (μ, u) . However, the fact that Lipschitz continuity is only local in μ , which is a consequence of the need to maintain coercivity of the diffusion equation (2a), prevents the extension of this result to larger times. Nevertheless we are able to identify a Lyapunov-candidate function, i.e., a function whose time derivative along the flow trajectories (its Lie derivative) is strictly negative and is equal to zero only when the it attains its minimum.

Next, on the basis of these findings, we experiment numerically the large time behavior of the proposed system (2) together with the extended dynamics (3). Given a triangulation of the domain Ω , the discrete model uses a \mathcal{P}_1 Galerkin approach for the discretization of the potential u and a \mathcal{P}_0 Galerkin scheme for the discretization of the diffusion coefficient μ . To avoid oscillations on the numerical

gradient, we use different approximation spaces for u and μ by defining the \mathcal{P}_1 potential on a uniformly refined mesh, an approach reminiscent of the inf-sup stable \mathcal{P}_1 -iso- $\mathcal{P}_2/\mathcal{P}_1$ Stokes FEM spaces. This methodology leads to a coupled differential algebraic system of equations that is solved by a simple forward Euler method. The resulting numerical algorithm is applied for the solution of the dynamics of *P. Polycephalum* on the maze.

The conjecture that problems (2) and (4) are asymptotically equivalent finds application to the numerical solution of the OT equations as, from preliminary experimental evidence, convergence to an asymptotic state seems smooth and fast even using the low order standard $\mathcal{P}_1/\mathcal{P}_0$ Galerkin approximations described above and on relatively coarse meshes. The conjecture is supported experimentally by comparing our numerical solution against the numerical results presented in Barrett and Prigozhin [4], where solution to (4) was obtained by means of RT0 mixed finite elements and automatic mesh refinement at on a larger triangulation and with much higher computational costs. Eventually, from a numerical point of view, the above asymptotic behavior seems rather robust under iterated mesh refinements.

2. MAIN RESULTS

In this Section we lay down the technical results about our slime mold dynamics gained in a rather sharp and convenient functional environment. The main idea consists on the synthesis of the proposed dynamics towards an infinite dimensional abstract ODE that passes through a standard elliptic setting. We obtain a theorem about local existence and uniqueness, but at present we are not able to extend this result to larger times. Nevertheless, an interesting Lyapunov function is inherited by invoking the analogy of our problem at infinite time with the PDE based Optimal Transport setting and its relationship with the shape optimization problem. Assuming existence of the solution and its first time derivative at all times, we prove that the Lyapunov-candidate function is always decreasing in time and reaches stationarity at $t = \infty$. Although we are not currently able to use it properly, this result seems promising in the search for a global existence theorem and a formal justification of the conjecture that the proposed slime-mold problem is, at infinite time, equivalent to the MK problem.

2.1. Notations. We will denote by \mathcal{F} the set of essentially bounded functions f with zero mean and compact support in an open, bounded, and convex and simply-connected subset Ω of \mathbb{R}^n :

$$\mathcal{F} := \left\{ f \in L^\infty(\Omega) : \text{supp}(f) \subsetneq \Omega \text{ and } \int_{\Omega} f \, dx = 0 \right\}.$$

Without loss of generality, we may redefine the domain of f by means of an n -dimensional ball $B(0, \bar{R})$ with \bar{R} sufficiently large so that $\Omega \subset B(0, \bar{R})$ and with $f = 0$ outside of Ω (in most cases of interest Ω can be an n -dimensional interval). We will still use the same symbol Ω to denote such subset. We define the subset \mathcal{D} of $\mathcal{C}^\delta(\bar{\Omega})$ as:

$$\mathcal{D} := \left\{ \mu \in \mathcal{C}^\delta(\bar{\Omega}) \text{ such that } \lambda(\mu) := \min_{x \in \Omega} \mu(x) \geq \alpha > 0 \right\},$$

where

$$\mathcal{C}^\delta(\bar{\Omega}) = \left\{ v : \bar{\Omega} \mapsto \mathbb{R} : v_{[\delta, \bar{\Omega}]} := \sup_{x \neq y} \frac{|v(x) - v(y)|}{|x - y|^\delta} < +\infty \right\}$$

$$\|v\|_{\mathcal{C}^\delta(\bar{\Omega})} := \sup_{\Omega} v + v_{[\delta, \bar{\Omega}]}$$

with $\delta \in]0, 1[$. We indicate with $\mathcal{C}^{1,\delta}(\bar{\Omega})$ the Hölder space of continuously differentiable functions with first derivatives in $\mathcal{C}^\delta(\bar{\Omega})$. In the proof of Theorem 1, we will be using the following characterization of the subspace \mathcal{D} . Given $0 < a < b < \infty$, the subspace \mathcal{D} can be re-defined as the union of open and convex subsets:

$$(6) \quad \mathcal{D} = \bigcup_{0 < a < b < +\infty} \mathcal{D}(a, b)$$

$$\mathcal{D}(a, b) := \{ \mu \in \mathcal{C}^\delta(\bar{\Omega}) \text{ such that } a < \lambda(\mu) \leq \|\mu\|_{\mathcal{C}^\delta(\bar{\Omega})} < b \}.$$

Standard results on regularity theory of elliptic PDEs [15] allow us to give the following definitions.

Definition 1 (Potential). *Let $\mu \in \mathcal{D}$ and $f \in \mathcal{F}$. The operator $\mathcal{U} : \mathcal{D} \mapsto \mathcal{C}^{1,\delta}(\bar{\Omega})$ maps μ into $\mathcal{U}(\mu)$, where $\mathcal{U}(\mu)$ is the unique weak solution of the elliptic equation (2a), i.e.*

$$\int_{\Omega} \mu \nabla u \cdot \nabla \varphi \, dx = \int_{\Omega} f \varphi \, dx \quad \forall \varphi \in H^1(\Omega),$$

$$\int_{\Omega} u \, dx = 0.$$

Definition 2 (Flux). *Let $\mu \in \mathcal{D}$ and $f \in \mathcal{F}$. The operator $\mathcal{Q} : \mathcal{D} \mapsto \mathcal{C}^\delta(\bar{\Omega})$ is defined as:*

$$\mu \mapsto \mathcal{Q}(\mu) := \mu |\nabla \mathcal{U}(\mu)|.$$

2.2. Local existence and a Lyapunov-candidate function. In this section we report the main results and developments that lead to the local well-posedness of the model and to the identification of the proposed Lyapunov-candidate function. We start by writing the weak formulation of system (2):

$$(7a) \quad \int_{\Omega} \mu(t, x) \nabla u(t, x) \nabla \varphi(x) \, dx = \int_{\Omega} f(x) \varphi(x) \, dx \quad \forall \varphi \in H^1(\Omega)$$

$$(7b) \quad \int_{\Omega} u(t, x) \, dx = 0$$

$$(7c) \quad \mu'(t, x) = \mu(t, x) |\nabla u(t, x)| - \mu(t, x)$$

$$(7d) \quad \mu(0, x) = \mu_0(x) \in \mathcal{D}$$

Definitions 1 and 2 allow us to substitute the potential $\mathcal{U}(\mu)$ into (7c) to obtain the following semilinear evolution equation:

$$(8) \quad \begin{aligned} \mu'(t) &= -\mu(t) + \mathcal{Q}(\mu(t)) \\ \mu(0) &= \mu_0 \in \mathcal{D} \end{aligned}$$

where the dependence on x has been omitted. Obviously, the pair $(\mu(t, x), u(t, x))$ can be reconstructed from $(\mu(t), \mathcal{U}(\mu(t)))$. The mild formulation of (8) is given by:

$$(9) \quad \mu(t) = e^{-t} \mu_0 + \int_0^t e^{s-t} \mathcal{Q}(\mu(s)) \, ds$$

The Banach-Caccioppoli fixed point theory states that local existence and uniqueness of (8) require that the operator $\mathcal{Q}(\mu)$ be locally Lipschitz continuous. We have the following:

Proposition 1. *The Potential and Flux operators \mathcal{U} and \mathcal{Q} are Lipschitz continuous and bounded in $\mathcal{D}(a, b)$ for all a and b , $0 < a < b < \infty$.*

In other words we have that for every $\mu \in \mathcal{D}(a, b)$,

$$(10) \quad \|\mathcal{U}(\mu)\|_{\mathcal{C}^{1,\delta}(\bar{\Omega})} \leq C_1(a, b)$$

$$(11) \quad \|\mathcal{Q}(\mu)\|_{\mathcal{C}^\delta(\bar{\Omega})} \leq C_2(a, b)$$

and there exist constants $L_{\mathcal{U}}(a, b)$ and $L_{\mathcal{Q}}(a, b)$ such that, for every $\mu_1, \mu_2 \in \mathcal{D}(a, b)$:

$$(12) \quad \|\mathcal{U}(\mu_1) - \mathcal{U}(\mu_2)\|_{\mathcal{C}^{1,\delta}(\bar{\Omega})} \leq L_{\mathcal{U}}(a, b) \|\mu_1 - \mu_2\|_{\mathcal{C}^\delta(\bar{\Omega})}$$

$$(13) \quad \|\mathcal{Q}(\mu_1) - \mathcal{Q}(\mu_2)\|_{\mathcal{C}^\delta(\bar{\Omega})} \leq L_{\mathcal{Q}}(a, b) \|\mu_1 - \mu_2\|_{\mathcal{C}^\delta(\bar{\Omega})}$$

The previous Proposition follows from the following:

Lemma 1. *Let $\mu \in \mathcal{D}$, $F_0 \in \mathcal{F}$, and $F = (F_i)_{(i=1,\dots,n)} \in [\mathcal{C}^\delta(\bar{\Omega})]^n$ and $u \in H^1(\Omega)$ be the unique solution of*

$$(14) \quad \begin{cases} \int_{\Omega} \mu \nabla u \cdot \nabla \varphi \, dx = \int_{\Omega} (F_0 \varphi + F \cdot \nabla \varphi) \, dx & \forall \varphi \in H^1(\Omega) \\ \int_{\Omega} u \, dx = 0 \end{cases}$$

Then $u \in \mathcal{C}^{1,\delta}(\bar{\Omega})$ and the following estimate holds:

$$(15) \quad \|\nabla u\|_{\mathcal{C}^\delta(\bar{\Omega})} \leq K_\delta(n, \Omega, \delta) K_\mu(\mu) (\|F_0\|_{L^\infty(\Omega)} + \|F\|_{\mathcal{C}^\delta(\bar{\Omega})})$$

where $K_\delta(n, \Omega, \delta)$ is a constant depending on the dimension n , the domain Ω , and the Hölder regularity δ of μ , and:

$$(16) \quad K_\mu(\mu) = K_\mu(\lambda(\mu), \|\mu\|_{\mathcal{C}^\delta(\bar{\Omega})}) = \frac{1}{\lambda(\mu)} \left(\frac{\|\mu\|_{\mathcal{C}^\delta(\bar{\Omega})}}{\lambda(\mu)} \right)^{\frac{n+\delta}{2\delta}}.$$

This lemma, whose proof is given in Section 4.6, extends classical results of regularity theory of elliptic equations with Hölder continuous coefficients by careful estimation of the dependence upon $\mu \in \mathcal{D}$ of the constants K_δ and K_μ [15, 20]. The latter result allows us to prove the main theorem of the paper:

Theorem 1. *Given $\mu_0 \in \mathcal{D}$ there exists $\tau(\mu_0) > 0$ such that the Cauchy Problem (8) admits a unique solution $\mu \in \mathcal{C}^1([0, \tau(\mu_0)]; \mathcal{C}^\delta(\bar{\Omega}))$. Moreover, this solution remains strictly greater than zero and:*

$$(17) \quad \lambda(\mu(t)) \geq e^{-t} \lambda(\mu_0)$$

for $t \in [0, \tau(\mu_0)[$.

This theorem suggests that there must be an interplay between μ and $\nabla \mathcal{U}$ that constrains the flux $|\mathcal{Q}|$ to remain bounded so that, under the hypotheses of Theorem (1), existence and uniqueness of the solution pair (μ, u) is expected for all times. However, such a global result seems out of reach within the current framework because the conclusions of Lemma 1 do not allow us to improve the local Lipschitzianity of \mathcal{U} and \mathcal{Q} . Nonetheless, local existence and uniqueness of the solution, albeit incomplete, offer a certain degree of confidence on the correctness of the model of the PP dynamics, and justify the use of numerical discretizations to supply credible evidence that the model is well-posed for all times.

A further indication that the problem is globally well-posed is provided by the fact that we have identified a Lyapunov-candidate function that could be used to constrain the problem. This function is derived by borrowing from results in the field of mass/shape optimization and considering its relationship with optimal transport problems. We start the derivation of the Lyapunov-candidate function by defining the shape optimization problem as described in Bouchitté et al. [7].

Assume to have two nonnegative functions f^+ and f^- in Ω , with $\int_{\Omega} f^+ = \int_{\Omega} f^-$, representing, e.g., the density of a given electric charge, and a fixed amount of a conductive material, described by a nonnegative function σ having unit mass. Interpreting Ω as an insulating medium, we ask the question how to optimally distribute the given conductive material so that the heating induced by the current flow from f^+ to f^- is minimal. In Bouchitté et al. [7] the authors consider the case where f^+ , f^- and σ are non-negative Radon measures and discuss the connection between the mass optimization problem and a generalized version of the MK equations. They proved that the optimal distribution of conductive material σ^* given f^+ and f^- is

the normalized optimal transport density μ^* of the MK equations with $f = f^+ - f^-$. In the case of $f \in \mathcal{F}$, these results together with those given in De Pascale and Pratelli [12] lead to the following formulation:

$$\min_{\sigma \in \mathcal{M}} \mathcal{E}(\sigma) = \frac{1}{2} \int_{\Omega} \sigma |\nabla \mathcal{U}(\sigma)|^2 \quad \mathcal{M} = \left\{ \sigma \in L^\infty(\Omega) : \int_{\Omega} \sigma \, dx = 1 \right\}$$

Recasting the shape optimization intuition into the framework of our formulation, it is natural to identify a density $\sigma(t) = (\mu(t) / \int_{\Omega} \mu(t) \, dx)$ that belongs to \mathcal{M} . Then, following our conjecture that $\mu(t) \rightarrow \mu^*$ as $t \rightarrow \infty$, it is natural to assume that $\sigma(t)$ should tend to σ^* , solution of the shape optimization problem. Noting that $\mathcal{U}(\sigma) = (\int_{\Omega} \mu \, dx) \mathcal{U}(\mu)$, we can define our Lyapunov-candidate function as:

$$(18) \quad \mathcal{L}(\mu) := \frac{1}{2} \int_{\Omega} \mu \, dx \cdot \int_{\Omega} \mu |\nabla \mathcal{U}(\mu)|^2 \, dx$$

Intuitively, we are looking for a density μ that gives the best trade off between the total mass, and thus the cost, of the transport infrastructure and the dissipated energy. In the large times limit, the above function \mathcal{L} evaluated along the trajectory $\mu(t)$ should tend to the minimum of (18) and its time derivative should always be negative. Thus, \mathcal{L} is a reasonable Lyapunov-candidate function, as the following theorem states:

Theorem 2. *The function $\mathcal{L} : \mathcal{D} \mapsto \mathbb{R}^+$ defined above is strictly decreasing in time along the solution $\mu(t)$ for $t \in [0, \tau(\mu_0)[$.*

The previous theorem leads to the following lemma:

Lemma 2. *For all $t \in [0, \tau(\mu_0)[$ the L^1 -norm of $\mu(t)$ and $\mathcal{Q}(\mu(t))$ are bounded by constants depending only on the initial data μ_0 .*

3. NUMERICAL SOLUTION

In this section we describe the numerical discretization used to find an approximate solution to the proposed model, and report the numerical results obtained solving the proposed model to simulate the Physarum Polycephalum dynamics on the maze. Next we report some numerical results aimed at justifying the conjecture that the solution of the proposed time-dependent model tends as time tends to infinity to the solution of the Monge-Kantorovich problem. To this aim, the model is applied to the solution of the OT problems proposed by Barrett and Prigozhin [4] and the numerical results are compared.

3.1. Spatial and temporal discretization. The numerical solution of eqs. (7) is obtained by means of the method of lines. We denote with $\mathcal{T}_h(\Omega)$ and $\overline{\mathcal{T}}_{2h}(\Omega)$ two regular triangulations of the domain Ω , where \mathcal{T}_h is obtained from $\overline{\mathcal{T}}_{2h}$ by connecting the edge mid-points. Indicating with N_{2h} , E_{2h} , and M_{2h} the number of nodes, edges, and triangles of mesh $\overline{\mathcal{T}}_{2h}$, respectively, we have that $N_h = N_{2h} + E_{2h}$ and $M_h = 4M_{2h}$. Spatial discretization is achieved using standard Galerkin finite elements by projecting eq. (7a) onto the finite dimensional space $V_h = \mathcal{P}_1(\mathcal{T}_h(\Omega)) = \text{span}\{\varphi_1(x), \dots, \varphi_{N_h}(x)\}$ of piecewise linear Lagrangian basis functions defined on $\mathcal{T}_h(\Omega)$ and eq. (7c) onto the finite dimensional space $W_h = \mathcal{P}_0(\overline{\mathcal{T}}_{2h}(\Omega))$ of piecewise constant functions. Following this approach, the spatially discrete potential $u_h(t, x)$

and diffusion coefficient $\mu_h(t, x)$ are written as:

$$u_h(t, x) = \sum_{l=1}^{N_h} u_l(t) \varphi_l(x) \quad \varphi_l \in V_h = \mathcal{P}_1(\mathcal{T}_h)$$

$$\mu_h(t, x) = \sum_{r=1}^{M_{2h}} \mu_r(t) \chi_r(x) \quad \chi_r(x) = \begin{cases} 1 & \text{if } x \in T_r \\ 0 & \text{if } x \notin T_r \end{cases} \quad T_r \in \mathcal{T}_{2h}$$

Thus the FEM method yields the following system of differential algebraic equations:

Find $(u_h, \mu_h) \in V_h \times W_h$ such that:

$$(19a) \quad a_{\mu_h}(u_h, \varphi_m) = \int_{\Omega} \mu_h \nabla u_h \cdot \nabla \varphi_m \, dx = \int_{\Omega} f \varphi_m \, dx \quad m = 1, \dots, N_h$$

$$(19b) \quad \int_{\Omega} u_h \, dx = 0$$

$$(19c) \quad \int_{\Omega} \mu'_h \chi_s \, dx = \int_{\Omega} \mu_h (|\nabla u_h| - k) \chi_s \, dx \quad s = 1, \dots, M_{2h}$$

$$(19d) \quad \int_{\Omega} \mu_h(0, \cdot) \chi_s \, dx = \int_{\Omega} \mu_0 \chi_s \, dx \quad s = 1, \dots, M_{2h}$$

Forward Euler time stepping discretizes eq. (19c) yielding a decoupled system of linear equations. Denoting with Δt_j the time-step size so that $t_{j+1} = t_j + \Delta t_j$ and writing $u_h^j \approx u_h(t_j, x)$ and $\mu_h^j \approx \mu_h(t_j, x)$, the final solution algorithm can be written as:

$$(20a) \quad a_{\mu_h^j}(u_h^j, \varphi_m) = (f, \varphi_m), \quad m = 1, \dots, N_h$$

$$(20b) \quad \mu_s^{j+1} = \mu_s^j \left(1 + \Delta t_j (|\nabla u_h^j|_s - k_s) \right), \quad s = 1, \dots, M_{2h}$$

where

$$a_{\mu_h^j}(u_h^j, \varphi_m) = \int_{\Omega} \mu_h^j \nabla u_h^j \cdot \nabla \varphi_m \, dx = \sum_{l=1}^{N_h} u_l^j \int_{\Omega} \mu_h^j \nabla \varphi_l \cdot \nabla \varphi_m \, dx$$

and

$$|\nabla u_h|_s = \frac{1}{|T_s|} \int_{T_s} |\nabla u_h| \, dx \quad k_s = \frac{1}{|T_s|} \int_{T_s} k \, dx \quad \mu_s^0 = \frac{1}{|T_s|} \int_{T_s} \mu_0 \, dx.$$

Eq. (20a) is a sparse system of linear equations of dimension N_h , and is solved by means of the incomplete Choleski preconditioned conjugate gradient with the variant proposed by Bochev and Lehoucq [5] to solve the corresponding semi-definite linear system arising in our pure Neumann problem. The $M_{2h} \times M_{2h}$ linear system described in eq. (19c) is diagonal and leads to (20b). To maintain the coercivity of the FEM bilinear form $a_{\mu_h^j}(\cdot, \cdot)$ we impose a lower bound on μ_h of 10^{-10} .

Remark 1. *The choice of the two different FEM spaces V_h and W_h , which resemble the inf-sup stable \mathcal{P}_1 -iso- $\mathcal{P}_2/\mathcal{P}_1$ FEM spaces for the Stokes equation [8], is dictated by the need to reduce or eliminate oscillations on the gradient $|\nabla u_h|$ that occur if different approximating spaces are used. Experimentally, in fact, we observed that in the case $(u_h, \mu_h) \in \mathcal{P}_1(\mathcal{T}_h) \times \mathcal{P}_0(\mathcal{T}_h)$ oscillations in ∇u_h appear and destroy convergence of the numerical solution. On the other hand, using the proposed approach $(u_h, \mu_h) \in \mathcal{P}_1(\mathcal{T}_h) \times \mathcal{P}_0(\mathcal{T}_{2h})$, which essentially is nothing else than a simple average of the solution gradient on the larger triangles, all the oscillations disappear.*

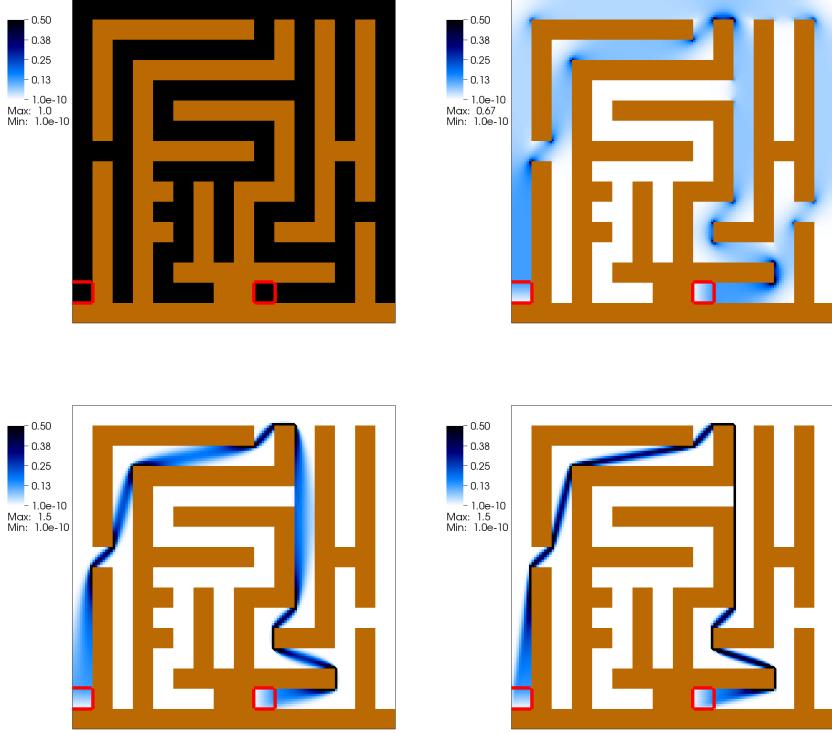


FIGURE 2. Simulation of the dynamics of *Physarum Polycephalum* mass reorganization in the maze experiment of Nakagaki et al. [17]: distribution of PP transport density at dimensionless times $t = 0$ (top, left), $t = 5.96$ (top, right), $t = 60.3$ (bottom, left), and $t = 9.6 \times 10^3$ (bottom, right). The simulation was done on a triangulation \mathcal{T}_{2h} with 32768 triangles and 16641 nodes. At the last time step of the simulation the μ_h variation was smaller than $\tau = 5 \times 10^{-9}$.

3.2. Numerical simulation of *Physarum Polycephalum* dynamics. The proposed model and its numerical discretization just described are applied to the simulation of the dynamics of the experiment described in Nakagaki et al. [17]. The domain encompassing the entire maze setup is discretized by means of a uniform triangulation obtained by subdividing each edge of the square-shaped maze into 128 subdivisions yielding the coarser mesh \mathcal{T}_{2h} comprised of 32768 elements and 16641 nodes. This high resolution is required to follow accurately the walls of the maze, which are described by setting $k(x) = 1000$ (brown colors in the upper left panel of Figure 2) while the maze paths are characterized by $k(x) = 1$. The initial condition μ_0 is set to 10^{-10} on the maze walls and one elsewhere. The two food sources $f^+ = 1$ and $f^- = -1$ are shown as red squares in the figure. We employ a variable time step size starting from $\Delta t_0 = 10^{-2}$ and with $\Delta t_{j+1} = \min(1.01\Delta t_j, 0.5)$, to ensure stability of the Forward Euler scheme is verified for all times with an ample safety margin. The simulation is stopped when the relative difference in μ_h becomes

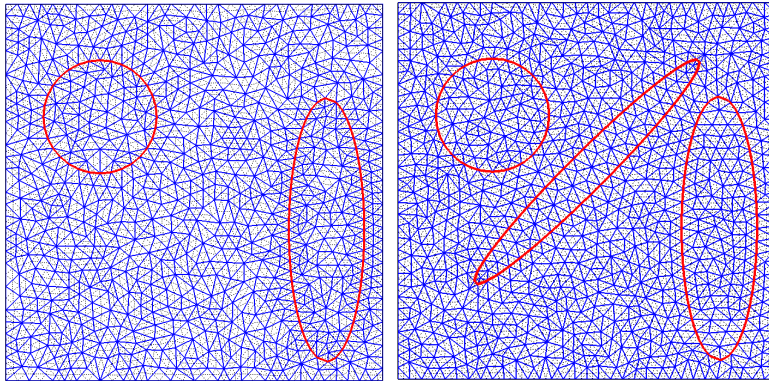


FIGURE 3. Unit square domain and triangulations \mathcal{T}_{2h} (solid blue) and \mathcal{T}_h (dotted black) for the homogeneous (left) and heterogeneous (right) test cases. The supports of f^+ (left circle) and f^- (right ellipse) are shown in red, as well as the central ellipse where $k(x)$ is different from the background in the heterogeneous case.

smaller than the tolerance τ , i.e.:

$$(21) \quad \text{var}(\mu_h(t^j)) = \frac{\|\mu_h^{j+1} - \mu_h^j\|_{L^2(\Omega)}}{\Delta t_j \|\mu_h^j\|_{L^2(\Omega)}} \leq \tau$$

with $\tau = 5 \times 10^{-9}$. Figure 2 shows the distribution of μ_h at three different times, in addition to the initial data. The three times are chosen in agreement with the simulations reported in Tero et al. [18] and are used to highlight the intermediate phases when the P.Polycephalum starts retreating from the dead ends ($t = 5.96$) and when it starts to concentrate along the identified shortest path ($t = 60.3$). The final steady state configuration is achieved at $t = 9.6 \times 10^3$. Note that the same numerical solution is obtained, albeit at different dimensionless times, starting from different initial conditions μ_0 . Looking at the first intermediate phase we see that PP has retreated from the dead end paths of the maze but persists on all the possible paths connecting the two food sources. We note a stronger concentration of μ_h at the edges of the maze walls, indicating that PP starts accumulating around a narrow band along the shortest route. This is clear from the solution at the next time (lower left panel), when the shortest path within the maze is completely identified but μ_h is still somewhat dispersed. At the final time, μ_h is distributed along the optimal route displaying varying approximation levels depending on the alignment of the mesh triangles with the support of μ_h . In fact, the vertical portion is one element thick, while the oblique routes encompass more than one triangle. All these observations are in line with the results proposed by Tero et al. [18], although in our case the graph structure is not imposed a-priori but it is mimicked through the appropriate definition of $k(x)$. Note that in our continuous setting the presence of $k(x)$ is related to the cost of through-flow, while the original graph-based formulation does allow only flow through the graph edges.

3.3. Numerical simulation of optimal transport problems. In this section we report numerical evidence supporting the conjecture that the long-time solution of the slime-mold dynamic model is solution of the Monge-Kantorovich equations (4). To this aim we compare our solution with the one proposed by Barrett and Prigozhin [4]. At the same time, the aim of this section is to show that the solution of the MK equations by means of the proposed dynamic model is numerically

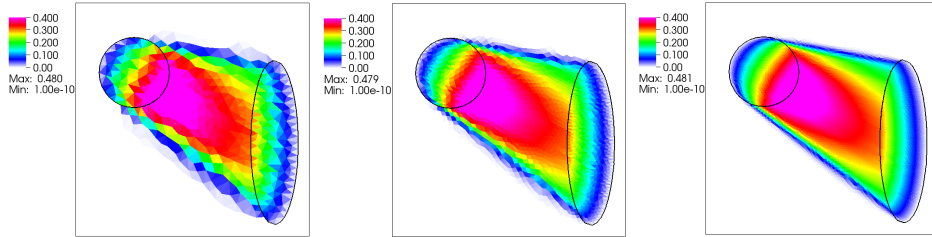


FIGURE 4. Numerical solution of the homogeneous OT problem: distribution of the transport density μ_h at three different mesh refinement levels of the coarser (\mathcal{T}_{2h}) triangulation (from left to right).

easier than the direct solution of system (4), suggesting that the introduction of time relaxes the numerical difficulties yielding a more robust, flexible, and efficient method for the numerical solution of optimal transportation problems.

We apply the numerical approach described above to the solution of the homogeneous and heterogeneous model problems proposed in Example 1 of Barrett and Prigozhin [4]. These problems consider a unit square domain with zero Neumann boundary and constant forcing having uniform positive value (f^+) supported on a circle and uniform negative value (f^-) on an ellipse in such a way that spatial balance is ensured (Figure 3). The domain contains a central oblique oval shape where a value for $k(x)$ different from the unitary background value is specified. Four different test cases are defined. The first one, called the homogeneous test case, considers a unit value of $k(x)$ assigned in the entire domain. This corresponds to the standard MK equation reported in system (4). Then three heterogeneous problems are addressed by setting the value of $k(x)$ in the central oblique ellipse equal to $k_e = 0.01$ and $k_e = 100$, respectively. The former case favors flow through the central oval, while the latter impedes it. The final test case considers an intermediate value of $k_e = 3$ in the central oval and is used to show the dynamical behavior of the proposed model by looking at the numerical solution at intermediate times.

To accurately impose the forcings of the different problems, the triangulations are adapted to the supports of $f(x)$ and $k(x)$, compelling the use of nonuniform meshes. The homogeneous case is solved on a sequence of three uniformly refined triangulation couples $\mathcal{T}_{2h}(\mathcal{T}_h)$. The coarsest mesh has 820(3170) nodes and 1531(6124) triangles (Figure 3, left), for a total of 4701(= 3170 + 1531) degrees of freedom in the final algebraic solution algorithm (20). The next two levels have 3170(12463) and 6124(24496) triangles, yielding a total of 18587 degrees of freedom, and 12463(49421) nodes and 24496(97984) triangles, for a total of 73917 degrees of freedom, respectively. In the heterogeneous case we employ two triangulation levels starting with a mesh of 933(3603) nodes and 1738(6952) elements (Figure 3, right). All simulations start with a spatially uniform unitary initial condition μ_h^0 and are run until condition (21) is satisfied with $\tau = 5 \times 10^{-9}$. The sequence of time step sizes is the same as in the case of the slime mold simulation, but with different upper bounds to ensure stability of Euler scheme at large times.

The experimental results for the homogeneous test case are shown in Figure 4, where the spatial distributions of μ_h^j and $|\nabla u_h^j|$ are plotted for the coarser (\mathcal{T}_h) mesh at the three refinement levels. All the features of the expected solution of the MK problem are present in these results, which are in good agreement with those of Barrett and Prigozhin [4]. The support of the transport density concentrates on the region connecting the circle boundaries with the ellipse. Along the transport rays, μ_h increases from zero to its maximum value within the supports of f^+ and

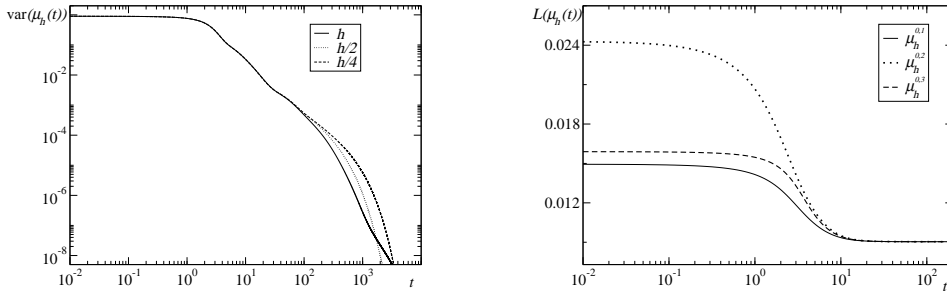


FIGURE 5. Numerical results for the homogeneous OT problem. Left panel: convergence towards zero of the relative variation of the transport density $\text{var}(\mu_h(t^j)) = \|\mu_h^{j+1} - \mu_h^j\|_{L^2(\Omega)} / (\Delta t_j \|\mu_h^j\|_{L^2(\Omega)})$ for the three refinement levels. Right panel: behavior of the Lyapunov function $\mathcal{L}(\mu_h(t^j))$ vs time for the three different initial data $(\mu_{h,1}^0, \mu_{h,2}^0, \mu_{h,3}^0)$ and the coarsest mesh level.

then decreases moving towards the ellipse, tending to negligible values at ray ends [9, 13]. The norm of the gradient, not shown for brevity, is practically one in all triangles of \mathcal{T}_{2h} lying within the support of μ_h . All these features are clearly visible already at the coarsest level, although the effects of large elements is evident. At increasing mesh refinements the delineation of the support of μ_h is sharper, and at the final level the accuracy seem to be satisfactory and compares well with the solution proposed by Barrett and Prigozhin [4].

Convergence toward steady state is monotonic, as shown in Figure 5 (left), where the relative variation of $\text{var}(\mu_h(t))$ (eq. (21)) is shown in log-log scale as a function of time for the three refinement levels. We notice that the convergence behavior is identical for all refinement levels up to a relative μ_h variation of approximately 10^{-3} , which corresponds to a dimensionless time $\hat{t} \approx 60$. At this point the discretization errors seem to slightly influence convergence. We note that from this time on the value of the Lyapunov candidate function (Figure 5, right panel) is practically constant, suggesting that the solution has effectively converged to a stationary state. At the first refinement level, the number of time steps to reach \hat{t} is 431, while 6641 is the number of time steps at the final time $t^* = 3200$ (the upper bound on Δt_j is 0.25). The average number of iterations of the IC0-preconditioned conjugate gradient per time-step is 66.

The model solution at large times is insensitive to the distribution of μ_h^0 as shown by the behavior of the Lyapunov function reported in the right panel of Figure 5, where three different sets initial data, $\mu_h^{0,i}$, $i = 1, 2, 3$, are tested:

$$\begin{aligned} \mu_{h,1}^0(x, y) &= 1 & \mu_{h,2}^0(x, y) &= 0.1 + 4((x - 0.5)^2 + (y - 0.5)^2) \\ \mu_{h,3}^0(x, y) &= 3 + 2 \sin(8\pi x) \sin(8\pi y) \end{aligned}$$

This result is upheld by the fact that the Lyapunov function $\mathcal{L}(\mu_h)$ numerically evaluated starting from three different initial conditions always converges to the same value (Fig. 5, right). Its non-increasing behavior shows that \mathcal{L} is a plausible candidate for a Lyapunov function.

In this work we are not interested in implementing the most computational efficient algorithm but we want to show that simple numerical methods are sufficient to find an accurate solution to the MK equations. We would like to remark that

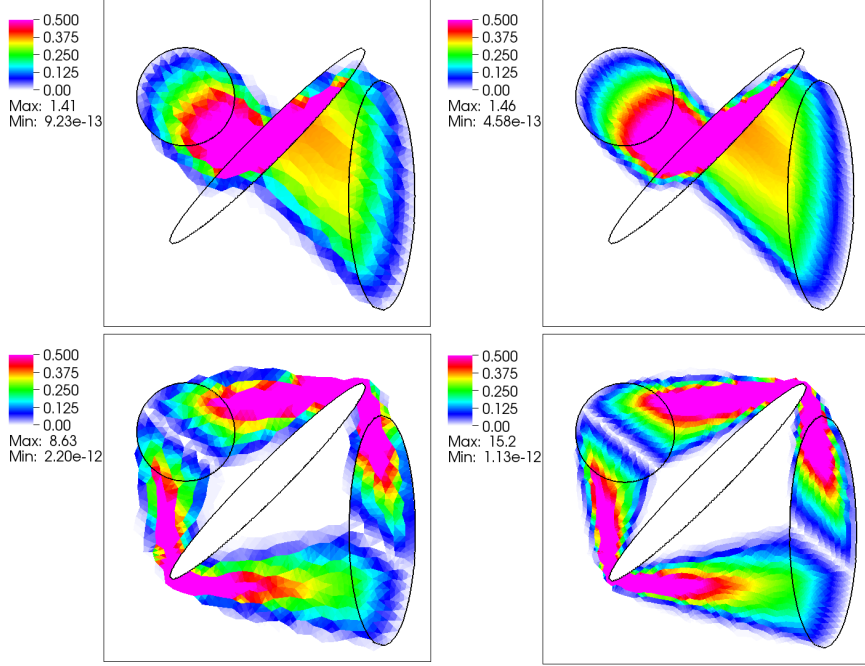


FIGURE 6. Numerical solution of the heterogeneous test case for $k_e = 0.01$ (top) and $k_e = 100$ (bottom) in the central ellipse. The figures show the optimal transport flux $\mu_h |\nabla u_h|$ for the mesh with 1738(6952) triangles and 933(3603) (left) and the once-refined mesh 6952(27808) triangles and 3603(14157) nodes (right).

many improvements can be done to the numerical scheme and are indeed under development. Notwithstanding its simplicity, our approach is competitive with respect to more direct MK solution methods, such as the one proposed in Barrett and Prigozhin [4]. These authors solve the direct optimal transport problem using a mixed finite element method with adaptive mesh refinement that converged to a final triangular grid adapted to the shape of the transport plan. The discretization on the final mesh level leads to a final nonlinear system with approximately 60000 degrees of freedom which is solved by an ad hoc nonlinear successive over-relaxation method. The Successive Over-relaxation method used to solve the nonlinear system was considered converged when the relative flux residual was smaller than 10^{-3} . Noting that in this case the convergence criteria based on relative variations of μ_h or on $q = \mu_h |\nabla u_h|$ are equivalent, as stated above, from Figure 5 we see that this convergence level is reached at $\hat{t} \approx 60$ in our case. At this time, our candidate Lyapunov function has reached an almost steady condition with a very small rate of decrease, signaling that for practical purposes convergence to the sought solution has been achieved.

The numerical results for the heterogeneous case are shown in Figure 6 where the steady-state spatial distribution of the absolute flux $q = \mu_h |\nabla u|$ is plotted in the case of $k_e = 0.01$ (top panels) and $k_e = 100$ (bottom panels). We first note that in this heterogeneous case the gradient is bounded by $k(x)$ and not by one as in the previous test case. For this reason we chose to plot the flux $|q| = \mu_h |\nabla u_h|$ instead of μ_h . Two successively refined triangulations are used, leading to linear systems of dimensions $N_h + M_{2h} = 3603 + 1738$ and $N_h + M_{2h} = 14157 + 6952 + 1738$ for the coarser and the finer meshes, respectively. The results

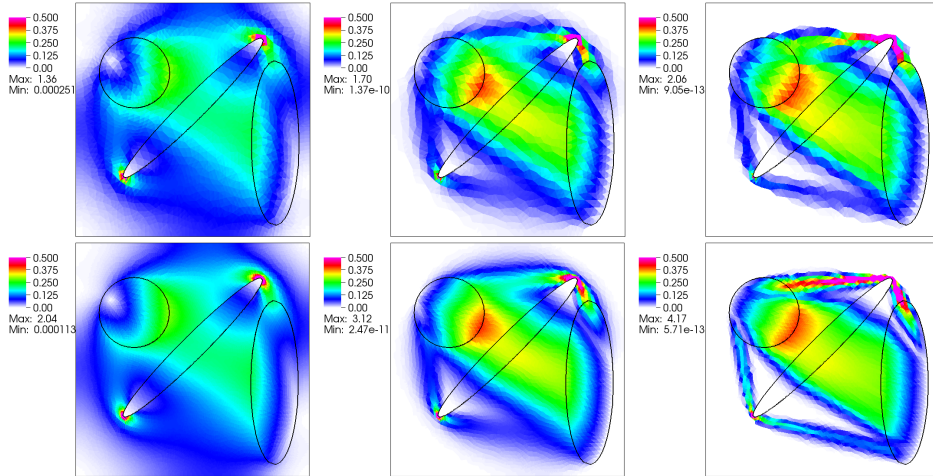


FIGURE 7. Numerical solution of the heterogeneous test case with $k_e = 3$ in the central ellipse in terms of optimal transport flux $\mu_h |\nabla u_h|$ for 3 different times ($\text{var}(\mu_h) = 0.1, 0.01, 5 \times 10^{-9}$ from left to right) and 2 refinement levels (from top to bottom).

are qualitatively comparable with those of Barrett and Prigozhin [4], although obtained with a much coarser discretization. It is interesting to note that the qualitative features of the solution are obtained already at the coarser mesh, with no visible numerical artifacts barring mesh roughness. We would like to stress here the fact that, notwithstanding the fact that the mesh nodes are not aligned with the support of μ_h , the geometrical features of the solution are well captured at all mesh resolution levels. From the flux spatial distribution, we see that values of k_e lower than one promotes larger fluxes across the central ellipses. On the contrary, values substantially larger than one restricts through-flow, and promotes the circumnavigation of the high low conductivity areas.

Finally, Figure 7 shows the distribution of μ_h for the case of $k_e = 3$ at three different times (left to right) and two successive refinement levels (top to bottom). The three times are chosen so that the μ_h variation reaches the thresholds $\text{var}(\mu_h(\hat{t}_1)) = 0.1$, $\text{var}(\mu_h(\hat{t}_2)) = 0.01$, and $\text{var}(\mu_h(\hat{t}_3)) = 5 \times 10^{-9}$. Correspondingly, we have $\hat{t}_1 \approx 5.2$ and $\hat{t}_2 \approx 21$, remaining the same for both tested triangulations, and $\hat{t}_3 = 1600$ for the coarser level and $\hat{t}_3 = 2200$ for the finer mesh as steady state is achieved at a later time for the finer mesh, reflecting the fact that the overall error is smaller. In fact, the converged steady state solution occurs after 6616 and 8955 time steps for the coarse and fine triangulations, respectively. Note that, for this last heterogeneous test case, the time-stepping sequence employed an upper bound on Δt_j equal to 0.25. Also in this case the steady-state numerical solution is similar to the results reported by Barrett and Prigozhin [4]. We see from the time sequence that our model constructs the transport map gradually. Starting from the uniformly distributed initial condition, it first identifies the larger flow paths and then refines them to arrive at the final configuration. The overall results are consistently pointing towards the veridicity of the conjecture that the infinite-time solution to our problem indeed coincides with the solution of the Monge-Kantorovich equations in the support of the optimal transport path.

4. PROOFS OF THE RESULTS

4.1. Proof of Proposition 1: Lipschitz continuity of \mathcal{U} and \mathcal{Q} . We start by considering the solution $u \in H^1(\Omega)$ of eq. (2a) in weak form:

$$(22) \quad \begin{cases} a_\mu(u, \varphi) = \int_\Omega \mu \nabla u \cdot \nabla \varphi \, dx = \int_\Omega f \varphi \quad \forall \varphi \in H^1(\Omega) \\ \int_\Omega u \, dx = 0 \end{cases}$$

We recall here the general hypotheses for the existence and uniqueness of the solution u of (22): i) the domain Ω be a bounded, connected, and convex subset of \mathbb{R}^n with C^1 or Lipschitz boundary $\partial\Omega$; ii) $f \in L^2(\Omega)$; iii) the bilinear form $a_\mu(u, \varphi)$ be bounded and coercive, i.e.:

$$(23) \quad \exists 0 < \Lambda < +\infty \quad \text{such that} \quad |a_\mu(u, v)| \leq \Lambda \|u\|_{H^1(\Omega)} \|v\|_{H^1(\Omega)} \quad \forall u, v \in H^1(\Omega)$$

$$(24) \quad \exists 0 < \lambda < +\infty \quad \text{such that} \quad a_\mu(u, u) \geq \lambda \|u\|_{H^1(\Omega)}^2 \quad \forall u \in H^1(\Omega)$$

It follows from the above that, if $\Omega = B(0, \bar{R})$, $\mu \in \mathcal{D}$, and $f \in \mathcal{F}$, the hypotheses for existence and uniqueness of the elliptic equation are satisfied and thus the operators \mathcal{U} and \mathcal{Q} are well defined. The regularity result provided in Lemma 1 ensures that \mathcal{U} maps into $C^{1,\delta}(\bar{\Omega})$. Then, given $\mu \in \mathcal{D}(a, b)$ we apply Lemma 1 with $F_0 = f$ and $F_i = 0$ to obtain:

$$(25) \quad \|\nabla \mathcal{U}(\mu)\|_{C^\delta(\bar{\Omega})} \leq K_\delta(\Omega, n, \delta) K_\mu(a, b) \|f\|_{L^\infty(\Omega)}$$

From this, the boundedness of the Potential $\mathcal{U}(\mu)$ follows immediately. The local Lipschitz continuity of \mathcal{U} derives from the following considerations. First, we note that given $\mu_1, \mu_2 \in \mathcal{D}(a, b)$ and $u_k = \mathcal{U}(\mu_k)$ with $k = 1, 2$, we have:

$$(26) \quad \begin{aligned} \int_\Omega \mu_1 \nabla u_1 \nabla \varphi \, dx &= \int_\Omega f \varphi \, dx = \int_\Omega \mu_2 \nabla u_2 \nabla \varphi \, dx \quad \forall \varphi \in H^1(\Omega) \\ \int_\Omega \mu_1 \nabla(u_1 - u_2) \nabla \varphi \, dx &= \int_\Omega (\mu_2 - \mu_1) \nabla u_2 \nabla \varphi \, dx \quad \forall \varphi \in H^1(\Omega) \end{aligned}$$

Then, application of Lemma 1 with $F_0 = 0$ and $F = -(\mu_1 - \mu_2) \nabla \mathcal{U}(\mu_2)$, which belongs to $(C^\delta(\bar{\Omega}))^n$ because of (25), yields:

$$(27) \quad \begin{aligned} \|\nabla(u_1 - u_2)\|_{C^\delta(\bar{\Omega})} &\leq K_\delta(\Omega, n, \delta) K_\mu(\mu_1) \|(\mu_1 - \mu_2) \nabla u_2\|_{C^\delta(\bar{\Omega})} \\ &\leq K_\delta(\Omega, n, \delta) K_\mu(\mu_1) \|\mu_1 - \mu_2\|_{C^\delta(\bar{\Omega})} \|\nabla u_2\|_{C^\delta(\bar{\Omega})} \\ &= K_\delta(\Omega, n, \delta)^2 K_\mu(a, b)^2 \|f\|_{L^\infty(\Omega)} \|\mu_1 - \mu_2\|_{C^\delta(\bar{\Omega})} \end{aligned}$$

We can also prove that the flux \mathcal{Q} is bounded in $\mathcal{D}(a, b)$. In fact, since the Hölder norm is sub-multiplicative, we can write from (25):

$$\|\mathcal{Q}(\mu)\|_{C^\delta(\bar{\Omega})} = \|\mu |\nabla \mathcal{U}(\mu)|\|_{C^\delta(\bar{\Omega})} \leq K_\delta(\Omega, n, \delta) b K_\mu(a, b) \|f\|_{L^\infty(\Omega)}$$

Lipschitz continuity of \mathcal{Q} derives from (27) as follows:

$$\begin{aligned} \|\mathcal{Q}(\mu_1) - \mathcal{Q}(\mu_2)\|_{C^\delta(\bar{\Omega})} &= \|\mu_1 |\nabla \mathcal{U}(\mu_1)| - \mu_2 |\nabla \mathcal{U}(\mu_2)|\|_{C^\delta(\bar{\Omega})} \\ &= \|\mu_1 (|\nabla \mathcal{U}(\mu_1)| - |\nabla \mathcal{U}(\mu_2)|) - (\mu_2 - \mu_1) |\nabla \mathcal{U}(\mu_2)|\|_{C^\delta(\bar{\Omega})} \\ &\leq \|\mu_1\|_{C^\delta(\bar{\Omega})} \|\nabla[\mathcal{U}(\mu_1) - \mathcal{U}(\mu_2)]\|_{C^\delta(\bar{\Omega})} \\ &\quad + K_\delta(\Omega, n, \delta) K_\mu(a, b) \|f\|_\infty \|\mu_1 - \mu_2\|_{C^\delta(\bar{\Omega})} \\ &\leq L_{\mathcal{Q}}(a, b) \|\mu_1 - \mu_2\|_{C^\delta(\bar{\Omega})} \end{aligned}$$

4.2. Proof of Theorem 1: local existence. Given $\mu_0 \in \mathcal{D}$ and the Lipschitz continuity of \mathcal{Q} in $\mathcal{D}(a, b)$ asserted by Prop. 1, noting that the subspace \mathcal{D} can be decomposed as given in (6), we may restrict our investigations on $\mathcal{D}(a, b)$. Standard arguments in the theory of ODEs in Banach Spaces ensure local existence and uniqueness of the solution $\mu(t)$. In other words, there exists a sufficiently small $\tau(\mu_0) > 0$ such that the fix point problem (9) admits a solution $\mu \in \mathcal{C}^0([0, \tau(\mu_0)]; \mathcal{C}^\delta(\bar{\Omega}))$. The Lipschitz continuity of \mathcal{Q} automatically ensures that $\mu \in \mathcal{C}^1([0, \tau(\mu_0)]; \mathcal{C}^\delta(\bar{\Omega}))$. The proof of estimate (17) is immediate by considering that in (9) the term $\int_0^t e^{s-t} \mathcal{Q}(\mu(s)) ds$ is always greater than zero.

4.3. Proof of Theorem 2: Lyapunov-candidate function. In this section we report the proof that Lyapunov-candidate function \mathcal{L} decreases along the trajectories. Before we compute the time derivative along the trajectories we need to prove the \mathcal{C}^1 -regularity in time of $u(t)$. We have the following (proof in Section 4.5):

Proposition 2. *The function $u(t)$ belongs to the space $\mathcal{C}^1([0, \tau(\mu_0)]; \mathcal{C}^{1,\delta}(\Omega))$. For each $t \in [0, \tau(\mu_0)[$ its time derivative $u'(t)$ solves the following equation:*

$$(28) \quad \begin{cases} \int_{\Omega} \mu(t) \nabla u'(t) \cdot \nabla \varphi dx = - \int_{\Omega} \mu'(t) \nabla u(t) \cdot \nabla \varphi dx & \forall \varphi \in H^1(\Omega) \\ \int_{\Omega} u'(t) dx = 0 \end{cases}$$

We can now compute the time derivative of $\mathcal{L}(\mu(t))$ and prove it is strictly negative, thus proving Theorem 2. In fact we have:

$$\begin{aligned} 2\mathcal{L}'(t) &= \frac{d}{dt} \left(\int_{\Omega} \mu(t) dx \int_{\Omega} \mu(t) |\nabla u(t)|^2 dx \right) \\ &= \int_{\Omega} \mu'(t) dx \int_{\Omega} \mu(t) |\nabla u(t)|^2 dx + \int_{\Omega} \mu(t) dx \frac{d}{dt} \int_{\Omega} \mu(t) |\nabla u(t)|^2 dx \\ &= \int_{\Omega} \mu'(t) dx \int_{\Omega} \mu(t) |\nabla u(t)|^2 dx + \int_{\Omega} \mu(t) dx \int_{\Omega} [\mu'(t) |\nabla u(t)|^2 \\ &\quad + 2 \mu(t) \nabla u'(t) \cdot \nabla u(t)] dx \end{aligned}$$

Substituting $\varphi = u(t)$ in (28) we get:

$$\int_{\Omega} \mu(t) \nabla u'(t) \cdot \nabla u(t) dx = - \int_{\Omega} \mu'(t) |\nabla u(t)|^2 dx$$

Thus

$$\begin{aligned} 2\mathcal{L}'(t) &= \int_{\Omega} \mu'(t) dx \int_{\Omega} \mu(t) |\nabla u(t)|^2 dx + \int_{\Omega} \mu(t) dx \int_{\Omega} [\mu'(t) |\nabla u(t)|^2 \\ &\quad - 2 \mu'(t) |\nabla u(t)|^2] dx \\ &= \int_{\Omega} \mu'(t) dx \int_{\Omega} \mu(t) |\nabla u(t)|^2 dx - \int_{\Omega} \mu(t) \int_{\Omega} \mu'(t) |\nabla u(t)|^2 dx \\ &= \int_{\Omega} \mu(t) (|\nabla u(t)| - 1) dx \int_{\Omega} \mu(t) |\nabla u(t)|^2 dx \\ &\quad - \int_{\Omega} \mu(t) dx \int_{\Omega} \mu(t) (|\nabla u(t)| - 1) |\nabla u(t)|^2 dx \\ &= \int_{\Omega} \mu(t) |\nabla u(t)| dx \int_{\Omega} \mu(t) |\nabla u(t)|^2 dx - \int_{\Omega} \mu(t) dx \int_{\Omega} \mu(t) |\nabla u(t)|^3 dx \end{aligned}$$

Rewriting the product of integrals as an integral in $\Omega \times \Omega$ of the functions

$$\begin{aligned} f(t; x, y) &:= \mu(t, x) |\nabla u(t, x)| \mu(t, y) |\nabla u(t, y)|^2 - \mu(t, x) \mu(t, y) |\nabla u(t, y)|^3 \\ g(t; x, y) &:= \mu(t, y) |\nabla u(t, y)| \mu(t, x) |\nabla u(t, x)|^2 - \mu(t, y) \mu(t, x) |\nabla u(t, x)|^3 \end{aligned}$$

we obtain:

$$\begin{aligned}
2\mathcal{L}'(t) &= \int_{\Omega \times \Omega} f(t; x, y) dx dy = \int_{\Omega \times \Omega} g(t; x, y) dx dy \\
&= \int_{\Omega \times \Omega} \frac{f(t; x, y) + g(t; x, y)}{2} dx dy \\
&= \int_{\Omega \times \Omega} \mu(t, x) \mu(t, y) \frac{h(t; x, y)}{2} dx dy
\end{aligned}$$

where

$$\begin{aligned}
h(t; x, y) &= |\nabla u(t, x)| |\nabla u(t, y)|^2 - |\nabla u(t, y)|^3 + |\nabla u(t, x)|^2 |\nabla u(t, y)| \\
&\quad - |\nabla u(t, x)|^3 \\
&= |\nabla u(t, x)| |\nabla u(t, y)| (|\nabla u(t, x)| + |\nabla u(t, y)|) \\
&\quad - (|\nabla u(t, x)|^3 + |\nabla u(t, y)|^3) \\
&= |\nabla u(t, x)| |\nabla u(t, y)| (|\nabla u(t, x)| + |\nabla u(t, y)|) \\
&\quad - (|\nabla u(t, x)| + |\nabla u(t, y)|) (|\nabla u(t, x)|^2 + |\nabla u(t, y)|^2) \\
&\quad - |\nabla u(t, x)| |\nabla u(t, y)| \\
&= - (|\nabla u(t, x)| + |\nabla u(t, y)|) (|\nabla u(t, x)|^2 + |\nabla u(t, y)|^2) \\
&\quad - 2|\nabla u(t, x)| |\nabla u(t, y)| \\
&= - (|\nabla u(t, x)| + |\nabla u(t, y)|) (|\nabla u(t, x)| - |\nabla u(t, y)|)^2
\end{aligned}$$

Finally, we arrive at:

$$\begin{aligned}
\mathcal{L}'(t) &= -\frac{1}{2} \int_{\Omega \times \Omega} \mu(t, x) \mu(t, y) (|\nabla u(t, x)| + |\nabla u(t, y)|) (|\nabla u(t, x)| - |\nabla u(t, y)|)^2 dx dy \\
&\leq 0
\end{aligned}$$

Remark 2. Note that, assuming global existence of the solution, $\mathcal{L}' = 0$ only if $\mu = 0$ or $|\nabla u| = \text{const}$ for all times. In particular, this assertion provides further support to our conjecture.

4.4. Proof of Lemma 2: boundedness of μ and \mathcal{Q} . The L^1 -bound for $\mathcal{Q}(\mu(t))$ derives directly from Theorem (2). By Cauchy-Schwartz inequality, we can write:

$$\begin{aligned}
\int_{\Omega} \mathcal{Q}(\mu(t)) dx &= \int_{\Omega} \mu(t)^{\frac{1}{2}} \mu(t)^{\frac{1}{2}} |\nabla \mathcal{U}(\mu(t))| dx \leq \left(\int_{\Omega} \mu(t) dx \int_{\Omega} \mu(t) |\nabla \mathcal{U}(\mu(t))|^2 dx \right)^{\frac{1}{2}} \\
&\leq \left(\int_{\Omega} \mu(0) dx \int_{\Omega} \mu(0) |\nabla \mathcal{U}(\mu(0))|^2 dx \right)^{\frac{1}{2}} = \mathcal{L}(\mu(0))^{\frac{1}{2}}
\end{aligned}$$

Then the L^1 -bound for $\mu(t)$ is obtained by integrating both sides of eq. (9) over Ω :

$$\begin{aligned}
\int_{\Omega} \mu(t) dx &= \int_{\Omega} \left(e^{-t} \mu_0 + \int_0^t e^{s-t} \mathcal{Q}(\mu(s)) ds \right) dx \\
&= e^{-t} \int_{\Omega} \mu_0 dx + e^{-t} \int_0^t e^s \left(\int_{\Omega} \mathcal{Q}(\mu(s)) dx \right) ds \\
&\leq e^{-t} \int_{\Omega} \mu_0 dx + e^{-t} \int_0^t e^s (\mathcal{L}(\mu_0))^{\frac{1}{2}} ds \\
&\leq \int_{\Omega} \mu_0 dx + (\mathcal{L}(\mu_0))^{\frac{1}{2}}
\end{aligned}$$

4.5. Proof of Proposition 2: \mathcal{C}^1 -regularity of $u(t)$. Let $t \in [0, \tau(\mu_0)[$ and choose $h > 0$ such that $t + h < \tau(\mu_0)$. The solution $\mu(t)$ of (8) belongs to a ball $B(\mu_0, R)$ centered in μ_0 and with appropriate radius R . More detailed information on the size of this R can be drawn from the proof of Theorem 1. Using (17), it is possible to find two constants $a(\mu_0), b(\mu_0)$ such that $\mu(t) \in \mathcal{D}(a(\mu_0), b(\mu_0))$. This allows us to write:

$$K_\mu(\mu(t)) = \frac{1}{\lambda(\mu(t))} \left(\frac{\|\mu(t)\|_{\mathcal{C}^\delta(\bar{\Omega})}}{\lambda(\mu(t))} \right)^{\frac{n+\delta}{2\delta}} \leq \frac{1}{a(\mu_0)} \left(\frac{b(\mu_0)}{a(\mu_0)} \right)^{\frac{n+\delta}{2\delta}} \quad \forall t \in [0, \tau(\mu)[$$

which shows that both the Potential and Flux operators are bounded and Lipschitz-continuous in $\mathcal{D}(a(\mu_0), b(\mu_0))$.

Heuristically, the proof is based on the observation that, assuming that both μ' and u' exist, we can take the derivative in time of (7a) and (7b) and use the fact that the source function is independent on time, thus obtaining (28). We first note that $u(t) = \mathcal{U}(\mu(t))$ is Lipschitz-continuous in time, since \mathcal{U} is locally Lipschitz-continuous and $\mu \in \mathcal{C}^1([0, \tau(\mu_0)[; \mathcal{C}^\delta(\bar{\Omega}))$. Next at each time $t \in [0, \tau(\mu_0)[$, we define $w(t)$, that heuristically should be $u'(t)$, as the unique solution of:

$$(29) \quad \begin{cases} \int_{\Omega} \mu(t) \nabla w(t) \cdot \nabla \varphi \, dx = - \int_{\Omega} \mu'(t) \nabla u(t) \cdot \nabla \varphi \, dx & \forall \varphi \in H^1(\Omega) \\ \int_{\Omega} w(t) \, dx = 0 \end{cases}$$

It is easy to verify that $w(t) \in \mathcal{C}^{1,\delta}(\bar{\Omega})$. Hence $\forall \varphi \in H^1(\Omega)$ we can write:

$$\int_{\Omega} \mu(t) \nabla u(t) \cdot \nabla \varphi \, dx = \int_{\Omega} f \varphi \, dx = \int_{\Omega} \mu(t+h) \nabla u(t+h) \cdot \nabla \varphi \, dx$$

Changing sign and adding in both sides $\int_{\Omega} \mu(t) \nabla u(t+h) \cdot \nabla \varphi \, dx$, yields:

$$(30) \quad \begin{aligned} \int_{\Omega} \mu(t) \nabla [u(t+h) - u(t)] \cdot \nabla \varphi \, dx = \\ - \int_{\Omega} [\mu(t+h) - \mu(t)] \nabla u(t+h) \cdot \nabla \varphi \, dx \end{aligned}$$

Now we multiply (29) by $-h$ and sum (29) and (30) to obtain:

$$\begin{aligned} & \int_{\Omega} \mu(t) \nabla [u(t+h) - u(t) - h w(t)] \cdot \nabla \varphi \, dx \\ &= - \int_{\Omega} [\mu(t+h) - \mu(t)] \nabla u(t+h) \cdot \nabla \varphi \, dx + h \int_{\Omega} \mu'(t) \nabla u(t) \cdot \nabla \varphi \, dx \\ &= - \int_{\Omega} \{ [\mu(t+h) - \mu(t) - h \mu'(t)] \nabla u(t+h) \\ & \quad + h \mu'(t) (\nabla u(t+h) - \nabla u(t)) \} \cdot \nabla \varphi \, dx \\ &= - \int_{\Omega} [G_1(t, h) + h G_2(t, h)] \cdot \nabla \varphi \, dx \end{aligned}$$

with

$$\begin{aligned} G_1(t, h) &= [\mu(t+h) - \mu(t) - h \mu'(t)] \nabla u(t+h) \\ G_2(t, h) &= \mu'(t) [\nabla u(t+h) - \nabla u(t)] \end{aligned}$$

Since $\mu \in \mathcal{C}^1(0, \tau; \mathcal{C}^\delta(\bar{\Omega}))$, we can estimate the above functions G_1 and G_2 as:

$$\begin{aligned} \|G_1(t, h)\|_{\mathcal{C}^\delta(\bar{\Omega})} &\leq \|\mu(t+h) - \mu(t) - h \mu'(t)\|_{\mathcal{C}^\delta(\bar{\Omega})} \|\nabla u(t+h)\|_{\mathcal{C}^\delta(\bar{\Omega})} \\ &\leq K_\delta(n, \Omega, \delta) K_\mu(\mu(t)) \|f\|_{L^\infty(\Omega)} \cdot o(h) \\ &\leq K_\delta(n, \Omega, \delta) K(\mu_0) \|f\|_{L^\infty(\Omega)} \cdot o(h) \end{aligned}$$

and, since the Potential operator is Lipschitz-continuous, we have also:

$$\begin{aligned} \|G_2(t, h)\|_{\mathcal{C}^\delta(\bar{\Omega})} &= \|\mu'(t) [\nabla u(t+h) - \nabla u(t)]\|_{\mathcal{C}^\delta(\bar{\Omega})} \\ &\leq \|\mu'(t)\|_{\mathcal{C}^\delta(\bar{\Omega})} \|\nabla u(t+h) - \nabla u(t)\|_{\mathcal{C}^\delta(\bar{\Omega})} \\ &\leq L(\mu_0)h \end{aligned}$$

where $L(\mu_0)$ is a function of f , K_δ . Thus we can write:

$$\|G_1 + hG_2\|_{\mathcal{C}^\delta(\bar{\Omega})} \leq \|G_1\|_{\mathcal{C}^\delta(\bar{\Omega})} + \|G_2\|_{\mathcal{C}^\delta(\bar{\Omega})} = o(h)$$

and, for Theorem 1 using $F = -(G_1 + hG_2)$, we obtain:

$$\lim_{h \rightarrow 0} \frac{\|\nabla[u(t+h) - u(t) - hw(t)]\|_{\mathcal{C}^\delta(\bar{\Omega})}}{h} = 0$$

that shows that $u' \in \mathcal{C}^1(0, \tau; \mathcal{C}^\delta(\bar{\Omega}))$ with $u' = w$.

4.6. Proof of Lemma 1: elliptic regularity. Lemma 1 is analogous to Theorem 5.19 of Giaquinta and Martinazzi [15] simplified to a scalar elliptic equation but extended to explicitly determine the dependence of the inequality constants upon μ . We will denote with C or c generic constants that may depend upon n , Ω , and the Hölder continuity exponent δ but are always independent of μ . We will use the following result adapted from Proposition 5.8 in Giaquinta and Martinazzi [15]:

Lemma 3 (Elliptic Decay). *Let $v \in H^1(\Omega)$ be any solution of*

$$(31) \quad \int_{\Omega} \nabla v \nabla \varphi \, dx = 0 \quad \forall \varphi \in H_0^1(\Omega)$$

then there exists a constant $c(n)$ such that:

$$(32) \quad \int_{B(x_0, \rho)} |\nabla v|^2 \, dx \leq c(n) \left(\frac{\rho}{R}\right)^n \int_{B(x_0, R)} |\nabla v|^2 \, dx$$

$$(33) \quad \int_{B(x_0, \rho)} |\nabla v - (\nabla v)_{x_0, \rho}|^2 \, dx \leq c(n) \left(\frac{\rho}{R}\right)^{n+2} \int_{B(x_0, R)} |\nabla v - (\nabla v)_{x_0, R}|^2 \, dx$$

for arbitrary balls $B(x_0, \rho) \Subset B(x_0, R) \Subset \Omega$.

Our case follows from the observation that the derivatives of v satisfy the weak form of Laplace equation (see also Ambrosio et al. [3], page 61). Note that the constant $c(n)$ depends only on the problem dimension n as we are considering Laplace equation.

We also use the following result from Lemma 5.13 in Giaquinta and Martinazzi [15] and Lemma 9.2 in Ambrosio [2]:

Lemma 4 (Iteration lemma). *Let $\phi : \mathbb{R}^+ \mapsto \mathbb{R}^+$ be a non-negative and non-increasing function satisfying*

$$(34) \quad \phi(\rho) \leq A \left[\left(\frac{\rho}{R}\right)^\alpha + \epsilon \right] \phi(R) + B R^\beta$$

for some $A, \alpha, \beta > 0$, with $\alpha > \beta$ and for all $0 < \rho \leq R \leq R_0$, where $R_0 > 0$ is given.

Then there exist constants $\epsilon_0 = \epsilon_0(A, \alpha, \beta)$ and $C = C(A, \alpha, \beta)$ such that

$$(35) \quad \text{if } \epsilon \leq \epsilon_0 = \left(\frac{1}{2A}\right)^{\frac{2\alpha}{\alpha-\beta}} \quad \text{then} \quad \phi(\rho) \leq C \left[\frac{\phi(R)}{R^\beta} + B \right] \rho^\beta.$$

The proof of Lemma 1 uses a classical bootstrap technique introduced by Campanato [10], Morrey Jr [16] and used more recently by Colombo and Mingione [11] to show the regularity of local minimizers of double phase variational integrals. The technique can be described by the following steps. First we consider a compact set $K \Subset \Omega$ and prove that $u \in L^{2,\nu}(K)$ for a suitable regularity exponent ν with $0 < \nu < n$. Then, $u \in \mathcal{L}^{2,n+2\delta}(K)$ where $L^{2,\nu}(K)$ and $\mathcal{L}^{2,n+2\delta}(K)$ are the Morrey and Campanato spaces, respectively. The results are extended to the entire domain by assuming enough regularity of $\partial\Omega$. This latter step is not reported in the following proof for brevity. Finally, the equivalence between the Campanato spaces $\mathcal{L}^{2,n+2\delta}(\Omega)$ and $\mathcal{C}^\delta(\bar{\Omega})$ is used to prove estimate (15) and to derive the expression of the constant K_μ given in (16). We recall that the norm of a function $u : \Omega \rightarrow \mathbb{R}^m$ (in our case we have either $m = 1$ or $m = n$) belonging to a Morrey space is given by:

$$\|u\|_{L^{2,\gamma}(\Omega)} = \left(\sup_{\substack{x_0 \in \Omega \\ \rho > 0}} \rho^{-\gamma} \int_{\Omega(x_0,\rho)} |u|^2 dx \right)^{\frac{1}{2}}$$

where $\Omega(x_0,\rho) = \Omega \cap B(x_0,\rho)$ and $0 \leq \gamma < n$. For $0 \leq \gamma < n + 2$, the norm of u belonging to a Campanato space is given by:

$$\|u\|_{\mathcal{L}^{2,\gamma}(\Omega)} = \|u\|_{L^2(\Omega)} + \left(\sup_{\substack{x_0 \in \Omega \\ \rho > 0}} \rho^{-\gamma} \int_{\Omega(x_0,\rho)} |u - (u)_{x_0,\rho}|^2 dx \right)^{\frac{1}{2}}$$

where $(u)_{x_0,\rho} = \int_{\Omega(x_0,\rho)} u dx / |\Omega(x_0,\rho)|$ is the average integral.

Proof. The first step of the bootstrap proceeds as follows. Consider $x_0 \in K$ and the ball $B_R := B(x_0, R) \Subset \Omega$. In this ball we use Korn's technique (freezing the coefficients) to decompose the solution as $u = v + w$ where $v \in H^1(B_R)$ satisfies the equations:

$$(36) \quad \int_{B_R} \mu(x_0) \nabla v \nabla \varphi dx = 0 \quad \forall \varphi \in H_0^1(B_R)$$

with $v = u$ in ∂B_R and the second equation is to be interpreted in the sense that $v - u \in H_0^1(B_R)$. The second function $w \in H_0^1(B_R)$ satisfies the equation:

$$(37) \quad \int_{B_R} \mu(x_0) \nabla w \nabla \varphi dx = \int_{B_R} \left[F_0 \varphi + F \cdot \nabla \varphi - (\mu(x) - \mu(x_0)) \nabla u \cdot \nabla \varphi \right] dx \quad \forall \varphi \in H_0^1(B_R)$$

with $w = 0$ in ∂B_R . Since $\mu(x_0)$ in (36) is a strictly positive and bounded scalar number it can be eliminated from the equation, hence w simply solves the weak form of Laplace equation:

$$(38) \quad \int_{B_R} \nabla v \nabla \varphi dx = 0 \quad \forall \varphi \in H_0^1(\Omega)$$

with $v = u$ in $\partial\Omega$. Thus we can use Lemma 3 to obtain:

$$(39) \quad \int_{B_\rho} |\nabla v|^2 dx \leq c(n) \left(\frac{\rho}{R} \right)^n \int_{B_R} |\nabla v|^2 dx$$

Recall that at this point our goal is to estimate the Morrey norm $\|\nabla u\|_{L^{2,\nu}(K)}$ with $\nu < n$. We use the above decomposition of u to estimate $\phi(\rho) := \int_{B_\rho} |\nabla u|^2 dx$,

$0 < \rho \leq R$. Thus we can write:

$$\begin{aligned}
\int_{B_\rho} |\nabla u|^2 dx &= \int_{B_\rho} |\nabla v + \nabla w|^2 dx \leq 2 \int_{B_\rho} |\nabla v|^2 dx + 2 \int_{B_\rho} |\nabla w|^2 dx \\
&\leq c(n) \left(\frac{\rho}{R}\right)^n \int_{B_R} |\nabla v|^2 dx + 2 \int_{B_\rho} |\nabla w|^2 dx \\
&= c(n) \left(\frac{\rho}{R}\right)^n \int_{B_R} |\nabla u - \nabla w|^2 dx + 2 \int_{B_\rho} |\nabla w|^2 dx \\
&\leq c(n) \left(\frac{\rho}{R}\right)^n \int_{B_R} |\nabla u|^2 dx + c(n) \left(\frac{\rho}{R}\right)^n \int_{B_\rho} |\nabla w|^2 dx \\
&\quad + 2 \int_{B_\rho} |\nabla w|^2 dx \\
&\leq c(n) \left(\frac{\rho}{R}\right)^n \int_{B_R} |\nabla u|^2 dx + c(n) \int_{B_R} |\nabla w|^2 dx
\end{aligned}$$

Note that, somewhat improperly, we always use the symbol $c(n)$ to indicate a constant depending on n only and that may assume different meaning even within the same equation. To estimate $\int_{B_R} |\nabla w|^2 dx$ we use $\varphi = w$ in (37) to get:

$$\begin{aligned}
(40) \quad \lambda(\mu) \int_{B_R} |\nabla w|^2 dx &\leq \int_{B_R} \mu(x_0) |\nabla w|^2 dx \\
&= \int_{B_R} [F_0 w + F \cdot \nabla w - (\mu(x) - \mu(x_0)) \nabla u \nabla w] dx
\end{aligned}$$

Using Hölder continuity of μ , and Poincaré and Cauchy-Scharwz inequalities, we can bound the right-hand-side of the previous equation to obtain:

$$\begin{aligned}
\int_{B(x_0, R)} F_0 w dx &\leq \|F_0\|_{L^2(B(x_0, R))} c(n) \|\nabla w\|_{L^2(B(x_0, R))} \\
\int_{B(x_0, R)} F \cdot \nabla w dx &\leq \|F\|_{L^2(B(x_0, R))} \|\nabla w\|_{L^2(B(x_0, R))} \\
\int_{B(x_0, R)} (\mu(x) - \mu(x_0)) \nabla u \nabla w dx &\leq R^\delta \|\mu\|_{C^\delta(\bar{\Omega})} \|\nabla u\|_{L^2(B(x_0, R))} \|\nabla w\|_{L^2(B(x_0, R))}
\end{aligned}$$

In the end, using Minkowski inequality to remove the double products, we can write:

$$\begin{aligned}
(41) \quad \int_{B_R} |\nabla w|^2 dx &\leq 2 \frac{1}{(\lambda(\mu))^2} \left[(c(n))^2 \|F_0\|_{L^2(B_R)}^2 \right. \\
&\quad \left. + \|F\|_{L^2(B_R)}^2 + R^{2\delta} \|\mu\|_{C^\delta(\bar{\Omega})}^2 \|\nabla u\|_{L^2(B_R)}^2 \right]
\end{aligned}$$

Since $F_0 \in L^\infty(\Omega)$, implying that $F_0 L^{2,\nu}(\Omega)$ and $\|F_0\|_{L^{2,\nu}(\Omega)}^2 \leq c(n) \|F_0\|_{L^\infty(\Omega)}^2$, we obtain:

$$(42) \quad \|F_0\|_{L^2(B_R)}^2 \leq c(n) \|F_0\|_{L^\infty(B_R)}^2 R^\nu \leq c(n) \|F_0\|_{L^\infty(\Omega)}^2 R^\nu$$

Since $F \in C^\delta(\bar{\Omega})$, each component of F belongs to $\mathcal{L}^{2,\gamma}(\Omega)$ for all $0 \leq \gamma \leq n + 2\delta$. Noting that we require $0 \leq \nu < n$, and in this case $L^{2,\nu}(\Omega) \equiv \mathcal{L}^{2,\nu}(\Omega)$, we obtain:

$$(43) \quad \|F\|_{L^2(B_R)}^2 \leq \|F\|_{\mathcal{L}^{2,\gamma}(B_R)}^2 R^\gamma \leq c(n) \|F\|_{C^\delta(\bar{\Omega})}^2 R^\gamma$$

Taking $\nu < n$ in (42) and $\gamma = \nu$ in (43) we get:

$$(44) \quad \int_{B_\rho} |\nabla u|^2 dx \leq c(n) \left[\left(\frac{\rho}{R} \right)^n + R^{2\delta} \left(\frac{\|\mu\|_{\mathcal{C}^\delta(\bar{\Omega})}}{\lambda(\mu)} \right)^2 \right] \int_{B_R} |\nabla u|^2 dx \\ + c(n) \left(\frac{\|F_0\|_{L^\infty(\Omega)}^2 + \|F\|_{\mathcal{C}^\delta(\bar{\Omega})}^2}{(\lambda(\mu))^2} \right) R^\nu$$

Now we rewrite inequality (44) in the form of the hypotheses of Lemma 4, i.e.:

$$\phi(\rho) := \int_{B_\rho} |\nabla u|^2 dx, \quad \alpha = n, \beta = \nu, \\ \epsilon = R^{2\delta} \left(\frac{\|\mu\|_{\mathcal{C}^\delta(\bar{\Omega})}}{\lambda(\mu)} \right)^2, \quad A = c(n), \quad B = c(n) \left(\frac{\|F_0\|_{L^\infty(\Omega)}^2 + \|F\|_{\mathcal{C}^\delta(\bar{\Omega})}^2}{(\lambda(\mu))^2} \right)$$

for $\rho \leq R$. Considering R such that:

$$R^{2\delta} \left(\frac{\|\mu\|_{\mathcal{C}^\delta(\bar{\Omega})}}{\lambda(\mu)} \right)^2 \leq \left(\frac{1}{2A} \right)^{\frac{2n}{n-\nu}} = A_0$$

we have that:

$$(45) \quad R \leq R_0 = A_0^{\frac{1}{\delta}} \left(\frac{\lambda(\mu)}{\|\mu\|_{\mathcal{C}^\delta(\bar{\Omega})}} \right)^{\frac{1}{\delta}}$$

We can now apply Lemma 4 to obtain, for $0 < \rho \leq R \leq R_0$, the following estimate:

$$(46) \quad \int_{B_\rho} |\nabla u|^2 dx \leq C(A, n, \nu) \rho^\nu \left(\frac{\int_{B_R} |\nabla u|^2 dx}{R^\nu} + B \right)$$

Incorporating all the constant into one single constant $C(n, \nu)$ we obtain:

$$(47) \quad \int_{B_\rho} |\nabla u|^2 dx \leq C(n, \nu) \rho^\nu \left(\frac{\int_{B_R} |\nabla u|^2 dx}{R^\nu} + \frac{\|F_0\|_{L^\infty(\Omega)}^2 + \|F\|_{\mathcal{C}^\delta(\bar{\Omega})}^2}{(\lambda(\mu))^2} \right)$$

The previous estimate is valid for every $B_R \Subset \Omega$. Varying $x_0 \in K$ and using the continuity inequality in the Lax-Milgram Lemma we obtain the desired estimate of this first step of the bootstrap procedure, i.e.:

$$(48) \quad \|\nabla u\|_{L^{2,\nu}(K)}^2 \leq C(n, \nu) \left(\frac{\int_{B_{R_0}} |\nabla u|^2 dx}{R_0^\nu} + \frac{\|F_0\|_{L^\infty(\Omega)}^2 + \|F\|_{\mathcal{C}^\delta(\bar{\Omega})}^2}{(\lambda(\mu))^2} \right) \\ \leq C(n, \nu) \left(\frac{C(\Omega) \|F_0\|_{L^\infty(\Omega)}^2 + \|F\|_{\mathcal{C}^\delta(\bar{\Omega})}^2}{(\lambda(\mu))^2} \frac{1}{R_0^\mu} + \frac{\|F_0\|_{L^\infty(\Omega)}^2 + \|F\|_{\mathcal{C}^\delta(\bar{\Omega})}^2}{(\lambda(\mu))^2} \right) \\ \leq C(n, \nu) C(\Omega) \frac{\|F_0\|_{L^\infty(\Omega)}^2 + \|F\|_{\mathcal{C}^\delta(\bar{\Omega})}^2}{(\lambda(\mu))^2} \left(\left(\frac{\|\mu\|_{\mathcal{C}^\delta(\bar{\Omega})}}{\lambda(\mu)} \right)^{\frac{\nu}{\delta}} + 1 \right) \\ \leq C(n, \nu) C(\Omega) \frac{\|F_0\|_{L^\infty(\Omega)}^2 + \|F\|_{\mathcal{C}^\delta(\bar{\Omega})}^2}{(\lambda(\mu))^2} \left(\frac{\|\mu\|_{\mathcal{C}^\delta(\bar{\Omega})}}{\lambda(\mu)} \right)^{\frac{\nu}{\delta}}$$

where $C(n, \nu)$ is bounded for all $\nu < n$.

The second step of the bootstrap procedure starts by noting that Equation (37) can be rewritten using $R = R_0$ as defined above:

$$(49) \quad \int_{B_R} \mu(x_0) \nabla w \nabla \varphi \, dx = \int_{B_R} \left[F_0 \varphi + (F - (F)_R) \cdot \nabla \varphi - \right. \\ \left. (\mu(x) - \mu(x_0)) \nabla u \cdot \nabla \varphi \right] dx \quad \forall \varphi \in H_0^1(B_R) \\ w = 0 \text{ in } \partial B_R$$

We continue by using again the decomposition $u = v + w$ and Lemma 3 to obtain:

$$\int_{B_\rho} |\nabla u - (\nabla u)_\rho|^2 \, dx = \int_{B_\rho} |\nabla v + (\nabla v)_\rho + \nabla w + (\nabla w)_\rho|^2 \, dx \\ \leq c(n) \left(\frac{\rho}{R} \right)^{n+2} \int_{B_R} |\nabla v - (\nabla v)_R|^2 \, dx + 2 \int_{B_\rho} |\nabla w - (\nabla w)_\rho|^2 \, dx \\ \leq c(n) \left(\frac{\rho}{R} \right)^{n+2} \int_{B_R} |\nabla u - (\nabla u)_R|^2 \, dx + c(n) \int_{B_R} |\nabla w|^2 \, dx$$

where the last inequality arises from the minimality of the mean. We follow the same developments as before, but now we explicitly include the factor R in the constant of Poincaré inequality to obtain:

$$(50) \quad \int_{B_\rho} |\nabla u - (\nabla u)_\rho|^2 \, dx \leq c(n) \left(\frac{\rho}{R} \right)^{n+2} \int_{B_R} |\nabla u - (\nabla u)_R|^2 \, dx \\ + 2c(n) \frac{R^2 \|F_0\|_{L^2(B_R)}^2 + \|F - (F)_R\|_{L^2(B_R)} + R^{2\delta} \|\mu\|_{C^\delta(\bar{\Omega})}^2 \|\nabla u\|_{L^2(B_R)}^2}{(\lambda(\mu))^2}$$

Since $\nabla u \in L^{2,\nu}(K)$ for $0 < \nu < n$ we can take $\nu = n - \delta$ in (48) to get:

$$\|\nabla u\|_{L^2(B_R)}^2 = \frac{\int_{B_R} |\nabla u|^2 \, dx}{R^{n-\delta}} R^{n-\delta} \leq \|\nabla u\|_{L^{2,n-\delta}} R^{n-\delta}$$

Using $\nu = n - 2 + \delta$ in (42) we obtain $\|F_0\|_{L^2(B_R)}^2 \leq c(n) \|F_0\|_{L^\infty(\Omega)} R^{n-2+\delta}$, while using $\gamma = n + \delta$ in (43) we have $\|F - (F)_R\|_{L^2(B_R)} \leq \|F\|_{C^\delta(\bar{\Omega})} R^{n+\delta}$. Substitution of these inequalities in (50) yields:

$$\int_{B_\rho} |\nabla u - (\nabla u)_\rho|^2 \, dx \leq c(n) \left(\frac{\rho}{R} \right)^{n+2} \int_{B_R} |\nabla u - (\nabla u)_R|^2 \, dx \\ + c(n) \frac{\|F_0\|_{L^\infty(\Omega)}^2 + \|F\|_{C^\delta(\bar{\Omega})} R^{n+\delta}}{(\lambda(\mu))^2} R^{n+\delta} \\ + R^{2\delta} \frac{\|\mu\|_{C^\delta(\bar{\Omega})}^2}{(\lambda(\mu))^2} C(n, n - \delta) C(\Omega) \frac{\|F_0\|_{L^\infty(\Omega)}^2 + \|F\|_{C^\delta(\bar{\Omega})}^2}{(\lambda(\mu))^2} \left(\left(\frac{\|\mu\|_{C^\delta(\bar{\Omega})}}{\lambda(\mu)} \right)^{\frac{n-\delta}{\delta}} \right) R^{n-\delta} \\ \leq c(n) \left(\frac{\rho}{R} \right)^{n+2} \int_{B_R} |\nabla u - (\nabla u)_R|^2 \, dx \\ + C(n, \Omega, \delta) \frac{\|F_0\|_{L^\infty(\Omega)}^2 + \|F\|_{C^\delta(\bar{\Omega})}^2}{(\lambda(\mu))^2} \left(1 + \frac{\|\mu\|_{C^\delta(\bar{\Omega})}^2}{(\lambda(\mu))^2} \left(\frac{\|\mu\|_{C^\delta(\bar{\Omega})}}{\lambda(\mu)} \right)^{\frac{n-\delta}{\delta}} \right) R^{n+\delta} \\ \leq c(n) \left(\frac{\rho}{R} \right)^{n+2} \int_{B_R} |\nabla u - (\nabla u)_R|^2 \, dx \\ + C(n, \Omega, \delta) \frac{\|F_0\|_{L^\infty(\Omega)}^2 + \|F\|_{C^\delta(\bar{\Omega})}^2}{(\lambda(\mu))^2} \left(\frac{\|\mu\|_{C^\delta(\bar{\Omega})}}{\lambda(\mu)} \right)^{\frac{n+\delta}{\delta}} R^{n+\delta}$$

Applying Lemma 4 with $\phi(\rho) := \int_{B_\rho} |\nabla u - (\nabla u)_\rho|^2 dx$ yields for $0 < \rho \leq R \leq R_0$:

$$\int_{B_\rho} |\nabla u - (\nabla u)_\rho|^2 dx \leq \rho^{n+\delta} C(n, \Omega, \delta) \cdot \left[\frac{\int_{B_R} |\nabla u - (\nabla u)_R|^2 dx}{R^{n+\delta}} + \left(\frac{\|F_0\|_{L^\infty(\Omega)}^2 + \|F\|_{\mathcal{C}^\delta(\bar{\Omega})}^2}{\lambda(\mu)^2} \right) \left(\frac{\|\mu\|_{\mathcal{C}^\delta(\bar{\Omega})}}{\lambda(\mu)} \right)^{\frac{n}{\delta}+1} \right]$$

from which, using again the minimality of the mean and the estimate of R_0 given in (45), we can evaluate:

$$\begin{aligned} \frac{\int_{B_\rho} |\nabla u - (\nabla u)_\rho|^2 dx}{\rho^{n+\delta}} &\leq C(n, \delta, \Omega) \cdot \left[\frac{\int_{B_{R_0}} |\nabla u - (\nabla u)_{R_0}|^2 dx}{R_0^{n+\delta}} + \left(\frac{\|F_0\|_{L^\infty(\Omega)}^2 + \|F\|_{\mathcal{C}^\delta(\bar{\Omega})}^2}{\lambda(\mu)^2} \right) \left(\frac{\|\mu\|_{\mathcal{C}^\delta(\bar{\Omega})}}{\lambda(\mu)} \right)^{\frac{n}{\delta}+1} \right] \\ &\leq C(n, \delta, \Omega) \left(\int_{B_{R_0}} |\nabla u - (\nabla u)_{R_0}|^2 dx + \frac{\|F_0\|_{L^\infty(\Omega)}^2 + \|F\|_{\mathcal{C}^\delta(\bar{\Omega})}^2}{\lambda(\mu)^2} \right) \left(\frac{\|\mu\|_{\mathcal{C}^\delta(\bar{\Omega})}}{\lambda(\mu)} \right)^{\frac{n}{\delta}+1} \\ &\leq C(n, \delta, \Omega) \left(\int_{\Omega} |\nabla u|^2 dx + \frac{\|F_0\|_{L^\infty(\Omega)}^2 + \|F\|_{\mathcal{C}^\delta(\bar{\Omega})}^2}{\lambda(\mu)^2} \right) \left(\frac{\|\mu\|_{\mathcal{C}^\delta(\bar{\Omega})}}{\lambda(\mu)} \right)^{\frac{n}{\delta}+1} \\ &\leq C(n, \delta, \Omega) \left(\frac{\|F_0\|_{L^\infty(\Omega)}^2 + \|F\|_{\mathcal{C}^\delta(\bar{\Omega})}^2}{\lambda(\mu)^2} \right) \left(\frac{\|\mu\|_{\mathcal{C}^\delta(\bar{\Omega})}}{\lambda(\mu)} \right)^{\frac{n}{\delta}+1} \end{aligned}$$

Hence $\nabla u \in \mathcal{L}^{2, n+\delta}(K)$ and we can write:

$$(51) \quad \|\nabla u\|_{\mathcal{L}^{2, n+\delta}(K)}^2 \leq C(n, \delta, \Omega) \left(\frac{\|F_0\|_{L^\infty(\Omega)}^2 + \|F\|_{\mathcal{C}^\delta(\bar{\Omega})}^2}{\lambda(\mu)^2} \right) \left(\frac{\|\mu\|_{\mathcal{C}^\delta(\bar{\Omega})}}{\lambda(\mu)} \right)^{\frac{n}{\delta}+1}$$

The bootstrap procedure is restarted from (49) using $\nu = n - 2 + 2\delta$ in (42) and $\gamma = n + 2\delta$ in (43), and estimate (51) in (50) so that a term $R^{n+2\delta}$ can be factored. Thus we can write:

$$\begin{aligned} \int_{B_\rho} |\nabla u - (\nabla u)_\rho|^2 dx &\leq c(n) \left(\frac{\rho}{R} \right)^{n+2} \int_{B_R} |\nabla u - (\nabla u)_R|^2 dx \\ &\quad + c(n) \frac{\|F_0\|_{L^\infty(\Omega)}^2 + \|F\|_{\mathcal{C}^\delta(\bar{\Omega})}^2}{(\lambda(\mu))^2} R^{n+2\delta} \\ &\quad + C(n, \delta, \Omega) \frac{\|F_0\|_{L^\infty(\Omega)}^2 + \|F\|_{\mathcal{C}^\delta(\bar{\Omega})}^2}{\lambda(\mu)^2} \left(\frac{\|\mu\|_{\mathcal{C}^\delta(\bar{\Omega})}}{\lambda(\mu)} \right)^{\frac{n}{\delta}+1} R^{n+2\delta} \end{aligned}$$

and finally, applying once again lemma 4, we have the final result:

$$(52) \quad \|\nabla u\|_{\mathcal{L}^{2, n+2\delta}(K)}^2 \leq C(n, \delta, \Omega) \frac{\|f\|_{L^\infty(\Omega)}^2 + \|G\|_{\mathcal{C}^\delta(\bar{\Omega})}^2}{\lambda(\mu)^2} \left(\frac{\|\mu\|_{\mathcal{C}^\delta(\bar{\Omega})}}{\lambda(\mu)} \right)^{\frac{n}{\delta}+1}$$

Extension of the previous estimate to the entire domain Ω can be obtained following the same bootstrap procedure starting from the analogue of the elliptic decay lemma 3 on hemispheres (similarly to what is proposed in Giaquinta and Martinazzi [15], Theorem 5.21). Such process introduces a dependence on the regularity of the boundary $\partial\Omega$ in the constant $C(n, \delta, \Omega)$ in (52), but we do not explicitly write such dependence. By the equivalence between $\mathcal{L}^{2, n+2\delta}(\Omega)$ and $\mathcal{C}^\delta(\bar{\Omega})$ we get:

$$\|\nabla u\|_{\mathcal{C}^\delta(\bar{\Omega})} \leq C(n, \delta, \Omega) \frac{\|F_0\|_{L^\infty(\Omega)} + \|F\|_{\mathcal{C}^\delta(\bar{\Omega})}}{\lambda(\mu)} \left(\frac{\|\mu\|_{\mathcal{C}^\delta(\bar{\Omega})}}{\lambda(\mu)} \right)^{\frac{n+\delta}{2\delta}}$$

which proves (15) and (16). From this, using Theorem 1.40 of Troianiello [20], we directly obtain that $u \in C^{1,\delta}(\bar{\Omega})$. \square

5. CONCLUSIONS

We have presented a continuous extension of the original model governing the dynamics of the Physarum Polycephalum slime mold. The proposed model couples an elliptic diffusion equation enforcing PP density balance with an ordinary differential equations governing the dynamics of the flow of information along the PP body. By transforming the problem into an infinite dimensional dynamical system, we are able to prove local in time existence and uniqueness of the problem solution under the hypothesis $L^\infty(\Omega)$ forcing function and Hölder continuous diffusion coefficient μ . Extension to larger (possibly infinite) times is not currently at reach, but the existence of a Lyapunov-candidate function and numerical evidence more seems to strongly justify our belief that a steady state solution to our model problem exists and that at this steady state conditions our model problem is equivalent to the PDE-based Monge-Kantorovich Optimal Transport problem. The Lyapunov-candidate function, which is characterized by a non-positive Lie derivative, is derived by recalling the analogy between the Monge-Kantorovich equations and shape optimization problems.

We describe a simple but rather efficient numerical formulation for the quantitative solution of our model problem and the simulation of the dynamics of Physarum Polycephalum. The numerical approach is based on a combination of piecewise constant a FEM discretization space for μ and a piecewise linear FEM space, defined on a once-refined triangulation, for the potential u . A simple forward Euler time discretization completes the discrete formulation. Preliminary numerical results show that the dynamics of the slime-mold is well captured, with all the features observed in the laboratory experiment reproduced in the virtual experimentation. Finally, we bring numerical evidence in support of the conjecture of equivalence between our dynamic problem and the Monge-Kantorovich equations by numerically solving classical Optimal Transport test cases [4]. The numerical results are in well agreement with the results shown in the literature and are obtained with a discretization scheme that is highly attractive for its remarkable computational attributes of simplicity and robustness.

ACKNOWLEDGMENTS

The authors are profoundly indebted with Giuseppe De Marco for his continuous stimulation and his important contributions during the development of this work.

REFERENCES

- [1] A. Adamatzky. *Physarum Machines*. Computers from Slime Mould. World Scientific, 2010.
- [2] L. Ambrosio. Lecture Notes on Optimal Transport Problems. In *Lecture Notes in Mathematics*, pages 1–52. Springer Berlin Heidelberg, Berlin, Heidelberg, 2004.
- [3] L. Ambrosio, A. Carlotto, and A. Massaccesi. *Lecture Notes on Partial Differential Equations*. <http://cvgmt.sns.it/paper/1280/>, 2010. URL <http://cvgmt.sns.it/paper/1280/>.
- [4] J. W. Barrett and L. Prigozhin. A mixed formulation of the Monge-Kantorovich equations. *Math. Model. Num. Anal.*, 41(6):1041–1060, 2007.
- [5] P. Bochev and R. B. Lehoucq. On the Finite Element Solution of the Pure Neumann Problem. *SIAM Rev.*, 47(1):50–66, Jan. 2005.

- [6] V. Bonifaci, K. Mehlhorn, and G. Varma. Physarum can compute shortest paths. *J Theor Biol*, 309:121–133, Sept. 2012.
- [7] G. Bouchitté, G. Buttazzo, and P. Seppecher. Shape optimization solutions via Monge-Kantorovich equation. *C. R. Acad. Sci. Paris Sér. I Math*, 324(10): 1185–1191, 1997.
- [8] F. Brezzi and M. Fortin. *Mixed and Hybrid Finite Element Methods*. Springer-Verlag, Berlin, 1991.
- [9] G. Buttazzo and E. Stepanov. On regularity of transport density in the monge-kantorovich problem. *SIAM J. Control Optim*, 42(3):1044–1055, 2003.
- [10] S. Campanato. Equazioni ellittiche del ii° ordine e spazi $\mathfrak{L}^{(2,\lambda)}$. *Annali di Matematica*, 69(1):321–381, 1965.
- [11] M. Colombo and G. Mingione. Bounded minimisers of double phase variational integrals. *Arch. Rational Mech. Anal.*, 218(1):219–273, Mar. 2015.
- [12] L. De Pascale and A. Pratelli. Sharp summability for monge transport density via interpolation. *ESAIM: COCV*, 10(4):549–552, Oct. 2004.
- [13] L. C. Evans and W. Gangbo. Differential equations methods for the Monge-Kantorovich mass transfer problem. *Mem. Am. Math. Soc.*, 137(653):0–0, 1999.
- [14] M. Feldman and R. J. McCann. Uniqueness and transport density in monge’s mass transportation problem. *Calc Var*, 15(1):81–113, 2002.
- [15] M. Giaquinta and L. Martinazzi. *An Introduction to the Regularity Theory for Elliptic Systems, Harmonic Maps and Minimal Graphs*. Springer Science & Business Media, Pisa, July 2013.
- [16] C. B. Morrey Jr. Second-order elliptic systems of differential equations. In *Contributions to the theory of partial differential equations*, pages 101–159. Princeton University Press, Princeton, N. J., 1954.
- [17] T. Nakagaki, H. Yamada, and A. Toth. Maze-solving by an amoeboid organism. *Nature*, 407(6803):470–470, 2000.
- [18] A. Tero, R. Kobayashi, and T. Nakagaki. A mathematical model for adaptive transport network in path finding by true slime mold. *J. Theor. Biol.*, 244(4): 553–564, Feb. 2007.
- [19] A. Tero, S. Takagi, T. Saigusa, K. Ito, D. P. Bebber, M. D. Fricker, K. Yumiki, R. Kobayashi, and T. Nakagaki. Rules for biologically inspired adaptive network design. *Science*, 327(5964):439–442, Jan. 2010.
- [20] G. Troianiello. *Elliptic Differential Equations and Obstacle Problems*. University Series in Mathematics. Springer, 1987.